



Published in final edited form as:

Biomaterials. 2010 June ; 31(18): 5007–5021. doi:10.1016/j.biomaterials.2010.02.075.

Transport and Biodistribution of Dendrimers Across Human Fetal Membranes: Implications for Intravaginal Administration of Dendrimers

Anupa R. Menjoge^{a,1,2}, Raghavendra S. Navath^{a,1,2}, Abbas Asad², Sujatha Kannan³, Chong Jai Kim², Roberto Romero², and Rangaramanujam M. Kannan^{1,2,*}

¹Department of Chemical Engineering and Material Science, and Biomedical Engineering, Wayne State University, Detroit, Michigan 48202

²Perinatology Research Branch, Eunice Kennedy Shriver National Institute of Child Health and Human Development, National Institutes of Health, and Department of Health and Human Services, Detroit, MI 48201

³Department of Pediatrics (Critical Care Medicine), Children's Hospital of Michigan, Wayne State University, Detroit, MI, 48201, USA

Abstract

Dendrimers are emerging as promising topical antimicrobial agents, and as targeted nanoscale drug delivery vehicles. Topical intravaginal antimicrobial agents are prescribed to treat the ascending genital infections in pregnant women. The fetal membranes separate the extra-amniotic space and fetus. The purpose of the study is to determine if the dendrimers can be selectively used for local intravaginal application to pregnant women without crossing the membranes into the fetus. In the present study, the transport and permeability of PAMAM (poly(amidoamine)) dendrimers, across human fetal membrane (using a side-by-side diffusion chamber), and its biodistribution (using immunofluorescence) are evaluated *ex-vivo*. Transport across human fetal membranes (from the maternal side) was evaluated using Fluorescein (FITC), an established transplacental marker (positive control, size~ 400 Da) and fluorophore-tagged G4-PAMAM dendrimers (~ 16 kDa). The fluorophore-tagged G4-PAMAM dendrimers were synthesized and characterized using ¹H NMR, MALDI TOF-MS and HPLC analysis. Transfer was measured across the intact fetal membrane (chorioamnion), and the separated chorion and amnion layers. Over a five hour period, the dendrimer transport across all the three membranes was less than < 3 %, whereas the transport of FITC was relatively fast with as much as 49% transport across the amnion. The permeability of FITC (7.9×10^{-7} cm²/s) through the chorioamnion was 7-fold higher than that of the dendrimer (5.8×10^{-8} cm²/s). The biodistribution showed that the dendrimers were largely present in interstitial spaces in the decidual stromal cells and the chorionic trophoblast cells (in 2.5 to 4 h) and surprisingly, to a smaller extent internalized in nuclei of trophoblast cells and nuclei and cytoplasm of stromal cells. Passive

© 2009 Elsevier Ltd. All rights reserved.

*Corresponding author: Rangaramanujam M. Kannan, Department of Chemical Engineering and Material Science, Wayne State University, Detroit, Michigan 48202; rkannan@eng.wayne.edu.

^aThese authors contributed equally to this manuscript.

Publisher's Disclaimer: This is a PDF file of an unedited manuscript that has been accepted for publication. As a service to our customers we are providing this early version of the manuscript. The manuscript will undergo copyediting, typesetting, and review of the resulting proof before it is published in its final citable form. Please note that during the production process errors may be discovered which could affect the content, and all legal disclaimers that apply to the journal pertain.

Appendix. Supplementary Data.

¹H NMR analysis of the intermediates and histology images are included.

diffusion and paracellular transport appear to be the major route for dendrimer transport. The overall findings further suggest that entry of drugs conjugated to dendrimers would be restricted across the human fetal membranes when administered topically by intravaginal route, suggesting new ways of selectively delivering therapeutics to the mother without affecting the fetus.

1. Introduction

A major challenge in drug therapy is to develop safe and selective targeting strategies in pregnancy [1]. Use of any drug during pregnancy is complicated by concerns of adverse effects on the pregnant women and the fetus [2]. Drugs administered orally to the mother reach the systemic circulation and have a potential to pass to the fetus [3]. In spite of the risk, there is a continuing need to receive medicines for genital infections (bacterial, yeast, herpes etc), epilepsy, diabetes, asthma and variety of other conditions during pregnancy[1,3]. Topical intravaginal microbicides are used to treat ascending genital infections in pregnant women[2,4-9]. Recently, dendrimers have been used as carriers[10], complexing agents[11], as encapsulating agents for topical microbicides [12] and as components of gel formulations[13-15]. The polylysine dendrimers (SPL7013) have emerged as topical antimicrobial agents for applications to the vaginal and cervical mucosa[16-19]. The VivaGel™ containing SPL7013 dendrimer is safe and well tolerated in human clinical trials [17] and further trials are being conducted to test its efficacy against genital herpes and HIV (human immunodeficiency virus). Optimization of prototype SPL7013 vaginal gel has been extensively evaluated [9,17,19]. Human clinical trials were conducted to determine the retention, duration of activity, safety and tolerability of SPL7013 gel applied intravaginally to young non-pregnant women [20]. Apart from SPL7013, the amine terminated PAMAM[21], carbosilane, poly(propyleneoxide) amine and ethylenediamine core dendrimers were found to exhibit antibacterial and antifungal activity[22-25]. Further, glycodendrimers have shown antimicrobial potential [26]. Therefore, understanding the transport and biodistribution of dendrimers in the placental membranes is being vital.

Over the years, the intravaginal or topical route of drug administration has emerged as an effective means for local delivery of antibacterials, antifungals, antiprotozoals, antivirals, labor-inducing and spermicidal agents, prostaglandins and steroids. To treat bacterial vaginosis in pregnant women, the intravaginal route is preferred over oral route to attain high local drug concentration in the vagina[27]. The commonly used preparations are clindamycin vaginal cream and topical metronidazole gel[5,7,27]. Topical application of imidazole and triazole agents are considered safe in pregnancy to treat yeast infections as these are minimally absorbed in the systemic circulation posing little risk of transfer to the fetus[2,6]. The intravaginal administration is preferred route to treat genital herpes in mother in last trimester of pregnancy while reducing the risk of neonatal herpes[17,28].

The use of topical microbicides is not limited to non-pregnant women and their use in pregnant women warrants their evaluation for transfer to the fetus and also to ensure the safety of mother and fetus. Previously, single intravaginal application of trimethoprim cream in pregnant women resulted in transfer of small but detectable amounts of trimethoprim into the amniotic fluid [29]. The diffusion of Terconazole across the amniotic membranes and exposure of the fetus on intravaginal administration is yet to be known [30]. Currently, Phase I clinical trials on pregnant women (HIV uninfected) are being conducted to evaluate the transfer of Tenofovir to the fetus after topical application of 1% vaginal gels, by measuring the plasma drug concentration, collection of placental and endometrial tissues, cord blood, and amniotic fluid [31,32] Dendrimers and other polymers are currently evaluated as topical intravaginal microbicides themselves or as a component of these formulations [4,9,31]. However, not much

is known about the transmembrane transport of these agents from the uterine cavity following the intravaginal application in pregnant women.

In light of the recent developments and extensive research directed towards evaluating the efficacy of different dendrimers as topical antimicrobial agents, it is prudent to understand their transport across the fetal membranes in order to extend their use as topical antimicrobials for treating infections in pregnant women, both from efficacy and fetal toxicology perspective. In the present study, we discuss transmembrane transport, permeability and biodistribution of dendrimers across human fetal membranes. Further, dendrimers are extensively investigated as components of several topical formulations [12,13,17,33,34], with potential for use in pregnant women. Therefore, their biodistribution pattern across fetal membranes needs to be evaluated. The fetal (chorioamniotic) membrane is a large temporary mucosal surface separating the amniotic cavity (fetus) and the extra-amniotic or uterine cavity [35]. The transport of a biocompatible, neutral, generation-4 PAMAM dendrimer (~16 kDa) and a small molecule, fluorescein isothiocyanate (FITC) (389 Da), across the human fetal membranes is evaluated in the present ex-vivo study. Immunofluorescent histological evaluation of the dendrimers at different time points was carried out to identify the transport mechanism, biodistribution and cellular uptake across these membranes.

2. Materials and methods

2.1. Materials

Ethylenediamine-core poly (amidoamine) [PAMAM] dendrimers (Diagnostic grade generation 4 with hydroxyl (OH) end groups) was purchased from Dendritech. Other reagents were obtained from assorted vendors in the highest quality available and include 4-(*tert*-Butoxycarbonylamino) butyric acid (Boc-GABA-OH, Aldrich), trifluoroacetic acid (TFA, Aldrich), Alexa Fluor 488 carboxylic acid, succinimidyl ester (Invitrogen, USA), Fluorescein isothiocyanate (FITC, Fluca), ethyl (dimethylaminopropyl) carbodiimide (EDC) (Sigma-Aldrich, USA) dimethyl sulphoxide (DMSO), dimethyl formamide (DMF). The solvents methanol and diethyl ether were purchased from Sigma-Aldrich and dialysis membrane (M.W cut off of 1000 Da) was purchased from Rancho Dominguez, CA, USA. The primary and secondary antibodies purchased were monoclonal mouse anti-human cytokeratin (M7018, Dako Carpinteria, CA, USA), rabbit polyclonal IgG vimentin (H-84) (sc5565, Santa Cruz Biotechnology Inc), Alexa Fluor®594 goat anti-mouse IgG (A11005, Invitrogen) and Alexa Fluor® 633 F(ab')₂ fragment of goat anti-rabbit IgG (A21072, Invitrogen).

2.2. NMR analysis

All ¹H NMR spectra were recorded on 400 MHz. The NMR chemical shifts are reported in ppm and calibrated against DMSO-*d*₆ (δ 2.48).

2.3. MALDI TOF-MS

MALDI-TOF/MS spectra were recorded on a bruker ultraflex system equipped with a pulsed nitrogen laser (337 nm), operating in positive ion reflector mode, using 19 kV acceleration voltage and a matrix of 2, 5 dihydroxybenzoic acid.

2.4. HPLC analysis

HPLC characterization of conjugates was carried out with Waters HPLC instrument equipped with two pumps, an auto sampler and dual UV and fluorescent detector interfaced to millennium software. The mobile phase used was acetonitrile / water (both 0.14% TFA by v/v) and water phase had a pH of 2.25. Mobile phases were freshly prepared, filtered and degassed prior to the use. Supelco discovery BIOwide pore C5 HPLC column (5 μm particle size, 25

cm × 4.6 mm length × I.D.) equipped with two C5 supelguard cartridges (5 μm particle size, 2 cm × 4.0 mm length × I.D.) was used for characterization of the conjugates. Gradient method was used for analysis and the mobile phase was water (100:0): acetonitrile to water-acetonitrile (60:40) in 25 minutes followed by returning to initial conditions in 15 minutes. The flow rate was 1 mL/min. The fluorescent detector was used at excitation 495 nm and emission 521 nm. The UV detector at 210 nm was used for detection of dendrimer prior to conjugation with fluorophore. All samples were analyzed in triplicate.

2.5. Synthesis of G₄-PAMAM-O-GABA-NHBoc (5)

The solution of Boc-GABA-OH (4) (914 mg, 4.50 mmol) in DMSO/DMF (3:1) was cooled to 0 °C and then added to the solution of EDC (860 mg, 4.50 mmol), DMAP (549 mg, 4.5 mmol) and G₄-PAMAM-OH (3) (1000 mg, 0.070 mmol) in DMSO/DMF (3:1). The reaction mixture was stirred at room temperature for 24 h. The reaction mixture was purified by dialysis with DMSO (24 h) to remove by-products and the excess of reactants. After dialysis the solvent was removed under lyophilization to get pure compound in 78 % yield (889mg, 0.055mmol). ¹H-NMR (DMSO-d₆, 400 MHz), δ (in ppm): 1.37(s, 9H), 1.50-1.66 (m, 2H), 2.10-2.20 (m, 4H), 3.97-4.03 (br s, 1H), 6.77-6.85 (br s, NH amide from GABA-NH-Boc), 7.70-8.05 (3 br s, NH amide from interior of dendrimer).

2.6. Synthesis of G₄-PAMAM-O-GABA-NH₂(6)

G₄-PAMAM-O-GABA-NHBoc (5) (1.0 g, 0.062mmol) was treated with trifloroacetic acid and dichloromethane (1:1, 10 mL). The reaction was stirred at room temperature for 10 min. After completion of the reaction, trifloroacetic acid / dichloromethane were removed under vacuum using rotavapor equipped with NaOH trap. Reaction mixture was neutralized with Na₂CO₃ and dialyzed with water (12 h) and solvent was removed under lyophilization to get pure compound (6) in 92 % yield (861mg, 0.057 mmol). ¹H-NMR (DMSO-d₆, 400 MHz), δ (in ppm): 1.65-1.78 (m, 2H), 2.2-2.39 (m, 4H), 3.91-3.99 (br s, 1H), 7.8-7.98 (br d, NH amide from GABA-NH₂), 8.03-8.25 (br d, NH amide from interior of dendrimer)

2.7. Synthesis of G₄-PAMAM-O-GABA-NH-FITC (1)

To a solution of G₄-PAMAM-O-GABA-NH₂ (6) (2.50 g, 0.167 mmol) in anhydrous DMSO (50 mL) was added fluorescein isothiocyanate (8) (FITC) (800 mg, 2.05 mmol) and stirred. The reaction was allowed to proceed further for 18 h at room temperature in dark. To remove unreacted FITC the reaction mixture was dialyzed (molecular cut off of the membrane is 1000 Da) in DMSO for 24 h. The compound was dissolved in methanol and precipitated in acetone. The product was dried by lyophilization to obtain G₄-PAMAM-O-GABA-NH-FITC (1) conjugate in the 75 % yield (1.98g, 0.125 mmol) and analyzed by ¹H-NMR and MALDI TOF / MS. Absence of free FITC in the conjugate was verified by TLC using chloroform and methanol (ratio 1:1) as mobile phase and further by HPLC analysis.

2.8. Synthesis of G₄-PAMAM-O-GABA-NH-Alexa-488 (2)

Alexa Fluor 488 carboxylic acid, succinimidyl ester (7) (2 mg, 0.0013 mmol) was added to a solution of G₄-PAMAM-O-GABA-NH₂ (6) (17.5 mg) in PBS (pH = 8) (3 mL) and the reaction was stirred at room temperature in dark for 15 h. The reaction mixture was dialyzed in DMSO (molecular cut off of the membrane is 1000 Da) for 24 h in dark. The product was dried by lyophilization to obtain G₄-PAMAM-O-GABA-NH-Alexa conjugate (2) in the yield 78 % (1.67 mg, 0.0001 mmol) and analyzed by MALDI TOF /MS. Absence of free Alexa in the conjugate was verified by TLC using chloroform and methanol (ratio 1:1) as mobile phase and further by HPLC analysis.

2.9. Dynamic light scattering measurements

Dynamic light scattering (DLS) analyses were performed using a Malvern Instruments Zetasizer Nano ZEN3600 instrument (Westborough, MA) with reproducibility being verified by collection and comparison of sequential measurements. G4-PAMAM-O-GABA-NH-FITC (1) and G4-PAMAM-O-GABA-NH-Alexa conjugate (2) samples were prepared using PBS pH = 7.4. DLS measurements were performed at a 90° scattering angle at 37 °C. Z-average sizes of three sequential measurements were collected and analyzed.

2.10. Chorioamniotic membrane specimens

2.10.1. Study design—All the human fetal (chorioamniotic) membrane samples were collected from women in uncomplicated normal pregnancies, immediately after elective caesarian section performed prior to the onset of labor. Fetal membrane samples were obtained from 21 normal pregnancies from the bank of biological samples of the Perinatology Research Branch. All women provided written informed consent before the collection of placenta and fetal membrane samples. The collection and use of tissue samples for research was approved by the Institutional Review Boards of the Eunice Kennedy Shriver National Institute of Child Health and Human Development at Wayne State University.

2.10.2. Chorioamniotic membrane processing—All human fetal membrane specimens were obtained at the time of cesarean section for obstetrical indications. The fetal membrane comprising chorioamniotic membrane (intact membranous tissue containing both amnion and chorion together) (n = 7) and amnion (n = 7) and chorion (n = 7) were separately procured (size 6 × 9"). Each membrane was cut into 9 pieces for the 9 sets of diffusion chamber. The fresh membranes were collected immediately after the delivery, washed with PBS to remove the blood and stored in PBS until (~1 h at 4 °C) it was mounted on the diffusion chamber (37 + 0.5 °C). Excess membranes were trimmed. The diffusion experiments were performed for 48 h by mounting the membrane in the chamber to study the transport across the membranes. In all the experiments with chorioamniotic membrane the choriodecidua (maternal side) was placed facing the donor chamber and the amnionic epithelium (fetal side) was facing the receptor chamber. The chorion and amnion were mechanically separated by gently pulling the two membranes apart. For the chorion, the side attached to amnion was placed facing the receptor chamber and for the amnion the side attached to the chorion was placed facing the donor chamber in the diffusion apparatus. For histological evaluation, the tissue samples were collected at 0.5, 1, 2, 3 and 4 h for and were fixed in 10 % formalin overnight. Further, some sections were analyzed by hematoxylin and eosin (H & E) staining. The membrane thickness was measured using the Mitutoyo Super Caliper by placing the respective membranes between the two glass slides and subtracting the thickness of the glass slides without the membrane.

2.10.3. Immunofluorescence—An immunofluorescence study was performed to investigate biodistribution of the dendrimer through the different layers of the fetal membrane with progression of time. The fetal membrane tissues were removed from the side by side diffusion chambers at different time points and fixed in 10 % formalin overnight. Double immunofluorescent staining was performed on 5 µm thick, paraffin sections of membranes placed on silanized slides. The different regions in the fetal membranes were identified based on the presence of trophoblast in the chorion as documented by staining with cytokeratin and the presence of the stromal cells as documented by staining with vimentin. The immunofluorescent staining was performed using Ventana Discovery autostainer for controlled and optimised reaction environment using the automation-optimized reagents from Ventana Medical Systems Inc. Briefly, paraffin wax sections were loaded onto the Ventana Discovery platform and following steps were completed automatically, these included dewaxing by EZ prep buffer (Ventana Medical Inc.), pre-treatment in Tris/EDTA pH 8.0 antigen retrieval solution (Ventana mCC1) or protease solution for 1 h (Ventana protease 2).

Endogenous peroxidase was inactivated using an enhanced inhibitor provided in the staining kit and nonspecific antibody binding was blocked by treatment with blocking solution for 10 min. The blocking solution was removed and the sections were washed three times with PBS/Tween solution incubated with primary antibodies for 1 h using the liquid cover slip (Ventana Medical Inc). The primary antibodies used were monoclonal mouse anti-human cytokeratin (1:200, M7018, Dako Carpinteria, CA, USA) and rabbit polyclonal IgG vimentin (H-84) (1:100, sc5565, Santa Cruz Biotechnology Inc). The sections were again washed three times with PBS/Tween solution incubated with secondary antibodies, Alexa Fluor®594 goat anti-mouse IgG (1:500, A11005, Invitrogen) and Alexa Fluor® 633 F(ab')₂ fragment of goat anti-rabbit IgG (1:500, A21072, Invitrogen) for 1 h using the antibody diluent from Ventana. The sections were washed with PBS/Tween, counterstained and mounted with DAPI prolong Gold antifade and cover slipped. Negative controls replaced primary antibodies with rabbit isotype control and mouse isotype controls (Invitrogen) in PBS. Images were captured from Leica TCS SP5 Laser Scanning Confocal Microscope (Leica Microsystems GmbH, Wetzlar, Germany). All study specimens were analyzed by a pathologist blinded to the clinical information.

2.10.4. In vitro permeability study—Permeation experiments were carried out using a two-chamber (donor and receptor) side-by-side Permeagear diffusion cell with a chamber volume of 3 mL and with a diameter of 13 mm and a diffusional area of 1.32 cm². The fetal membranes (chorion and amnion together, amnion and chorion) each (n = 9) were mounted between two halves of the donor and receptor cell (9 sets), which were further clamped together and sealed tightly with the rubber packing at the end of each glass chamber. The receptor cell (volume 3 mL) was filled with sterile PBS (pH 7.4). The donor cell (volume 3 mL) was filled with solution of compounds whose permeability was evaluated. The solutes chosen for the permeation study were FITC (MW = 389 Da), G₄-PAMAM dendrimers (G₄-PAMAM-O-GABA-Alexa (**2**), Mw = ~16 kDa and G₄-PAMAM-O-GABA-FITC (**1**), Mw = ~15.8 kDa). The system was maintained at 37 °C by using a circulating water bath and a jacket surrounding each cell. The donor and receiving medium was continuously stirred (600 rpm) with a magnetic bar to avoid stagnant aqueous diffusion layer effects. Aliquots (200 µL) were collected from the receptor cell every 30 min till first 6 h and at predetermined intervals thereafter and replaced with equal volume of PBS to maintain sink conditions throughout the study. The concentration of the solutes used were G₄-PAMAM-O-GABA-Alexa (0.6 mg/mL), G₄-PAMAM-O-GABA-FITC (3 mg / mL and 0.6 mg/mL), and FITC (0.3 mg/mL). The concentration of compound in the receptor medium was determined using a Molecular Devices SpectroMax M2, UV visible and Fluorescent plate reader at *ex* 495 / *em* 521. The cumulative amount of compound transported across the membrane in the receptor cell was determined using a calibration curve (a transport of 50% corresponds equilibrium achieved). All the experiments were conducted in dark room. All experiments were done in triplicate and the results are reported as mean ± STDev.

3. Results and discussion

A variety of *in-vitro* approaches have been used to assess the transport and permeation characteristics of drugs administered by different routes, such as permeability across the skin for topical formulations and permeability across the intestine, colon and jejunum for orally administered drugs [36]. Recently, dendrimers have been considered for topical applications to the vaginal and cervical mucosa as antimicrobial agents [16-19]. The fetus is separated from the extra-amniotic space in the uterus by the fetal membranes [35] and the ascending genital infections in pregnant women are treated by topical intravaginal application of antibacterial and antifungal drugs [2,4-9]. Since the dendrimers are explored as topical antimicrobial agents themselves and also as components of topical gel formulations, we have evaluated the transport, permeation and biodistribution of dendrimer across the human fetal

membranes (transmembrane transport) in the present study. The present study differs from the transplacental transport, where the transport of molecules or drugs across the placenta is evaluated and is relevant for substances present in systemic circulation of mother following administration by oral, parenteral or any other route [3,37,38]. The purpose of the present study is to determine whether (a) dendrimers on topical application to vagina and extra-amniotic cavity in pregnant women cross the fetal membrane and (b) could the dendrimers be used for site specific (local) activity and as components of topical delivery systems in pregnant women without crossing the fetal membranes and affecting the fetus.

3.1. Preparation of FITC-labeled G₄-PAMAM-O-GABA-NH₂ dendrimer (1)

The FITC labeled dendrimer was synthesized to evaluate its transport across human fetal membranes. To conjugate FITC (8) to G₄-PAMAM dendrimer with hydroxyl terminations (3), the linker GABA (4) with the amine groups protected with Boc (*tert*-butoxycarbonyl) was appended to the dendrimer to yield G₄-PAMAM-O-GABA-NHBoc (5). First, 4-(*tert*-butoxycarbonylamino) butyric acid (4) was reacted with G₄-PAMAM-OH (3) to give G₄-PAMAM-O-GABA-NHBoc (5) (Scheme-1) and the product so obtained was purified by dialysis using DMSO (cutoff 1000 Da). The ¹H NMR spectrum shows the appearance of characteristic signals of G₄-PAMAM-O-GABA-NHBoc at 1.37 (s, 9H), 1.50-1.66 (m, 2H) 2.10-2.20 (m, 4H), 3.97-4.03 (br s, 1H), 6.77-6.85 (br s, NH amide from GABA-NHBoc), 7.70-8.05 (3 br s, NH amide from interior of dendrimer) (Fig. S1. Supporting Information). This confirms the formation of G₄-PAMAM-O-GABA-Boc (5) product. It is evident from the integral ratio of the amide protons of G₄-PAMAM-O-GABA-NHBoc (5) at 7.70-8.05 ppm to the four methylene protons of GABA at 2.10-2.20 (m, 4H), that each G₄-PAMAM-OH dendrimer contains approximately 10 copies of GABA-NHBoc (4) molecules attached to it. The molecular weight of GABA-NHBoc (4) is 203 Da and the increment in mass of G₄-PAMAM dendrimer (from ~14 kDa) to 15960 Da as observed from MALDI TOF MS analysis further confirms the attachment of approximately 10 copies of GABA-NHBoc (4) to the dendrimer (Fig. 1). The product so obtained was deprotected to remove *tert*-butoxycarbonyl groups by treatment with trifluoroacetic acid in dichloromethane to obtain the amine-terminated G₄-PAMAM-O-GABA-NH₂ dendrimer (6). ¹H NMR spectrum shows the disappearance of characteristic signals at 1.37 ppm corresponding to *tert*-butoxycarbonyl after the deprotection step. Further, the spectrum shows presence of methylene protons at 1.65-1.78 (m, 2H) 2.2-2.39 (m, 4H) and amide protons at 7.8-7.98 (br d, NH amide from GABA-NH₂), 8.03-8.25 (br d, NH amide from interior of dendrimer) confirming the desired product G₄-PAMAM-O-GABA-NH₂ (6) (Fig. S2. Supporting Information). The MALDI-TOF / MS analysis of G₄-PAMAM-O-GABA-NH₂ (6) shows mass corresponding to 14,949 Da (Fig. 1). The mass of GABA is 103 Da suggesting an attachment of 10 molecules of GABA on G₄-PAMAM-O-GABA-NH₂ (6) (MALDI showed mass of G₄-PAMAM-OH as ~14 kDa (data not shown)).

The G₄-PAMAM-O-GABA-NH₂ dendrimer (6) was tagged with fluorescent dye FITC (8) as shown in Scheme 1. The FITC-labeled compound (G₄-PAMAM-O-GABA-NH-FITC) (1) was purified by dialysis (membrane cutoff 1000 Da) against DMSO in dark by replacing DMSO, to remove un-reacted compounds. Purity of G₄-PAMAM-O-GABA-NH-FITC (1) conjugate was confirmed by HPLC using fluorescent detector ($\lambda_{ex} = 495\text{nm} / \lambda_{em} = 521\text{nm}$). The G₄-PAMAM-O-GABA-NH-FITC conjugate (1) showed a single peak at 17.5 min in the reverse phase HPLC chromatogram indicating absence of free FITC in the conjugate after dialysis (Fig. 2). The stability of the conjugate in PBS (pH 7.4) after 72 h was evaluated by HPLC analysis which showed a single peak for the conjugate (1) and FITC was not released from the conjugate. This observation is consistent with previous reports where drugs conjugated to dendrimers by amide linkage are not released by hydrolytic or enzymatic degradation [39]. ¹H-NMR was used to characterize the conjugate. ¹H-NMR spectrum shows the appearance of aromatic protons at 6.47-6.59 (d, 6H, Ar) and 6.61-6.72 (s, 3H Ar) corresponding

to the FITC protons confirming the tagging of FITC on G₄-PAMAM-O-GABA-NH₂. The MALDI TOF / MS spectrum showed that the mass of G₄-PAMAM-GABA-NH₂ (**6**) increased from 14,949 Da to 15,805 Da suggesting the attachment of 2 molecules of FITC on G₄-PAMAM-O-GABA-NH-FITC (**1**) (Fig. 1).

3.2. Synthesis of G₄-PAMAM-O-GABA-Alexa conjugate (**2**)

G₄-PAMAM-O-GABA-NH₂ (**6**) dendrimer was reacted with the Alexa 488 carboxylic acid succinimidyl ester (**7**) (Scheme-1). The *N*-succinimidyl activated ester of Alexa 488 (**7**) couples to the terminal primary amines to yield amide-linked G₄-PAMAM-O-GABA-Alexa conjugate (**2**). The formation of conjugate (**2**) was confirmed by HPLC (Fig. 2) using fluorescent detector ($\lambda_{ex} = 495\text{nm}$ / $\lambda_{em} = 521\text{nm}$). The G₄-PAMAM-O-GABA-NH-Alexa conjugate (**2**) showed a single peak at 15.5 min in the reverse phase HPLC chromatogram. The absence of any other peak in chromatogram after dialysis of product confirms the absence of free alexa. Further, the stability of the conjugate in PBS (pH 7.4) after 72 h was evaluated by HPLC analysis which showed a single peak for the conjugate and alexa was not released from the conjugate. The MALDI spectrum showed that the mass of G₄-PAMAM-GABA-NH₂ (**6**) increased from 14,949 Da to 16065 Da confirming the attachment of 2 copies of alexa on G₄-PAMAM-O-GABA-NH-Alexa (**2**) (Fig. 1). The dendrimer alexa conjugate (**2**) was prepared for enhanced histological visualization of samples as confocal imaging causes quenching and also to match with the intensities of other alexa conjugated secondary antibodies.

3.3. Transmembrane transport of G₄-PAMAM dendrimer (**1**)

The dendrimer (**1**) transport and permeability was determined from chorioamnion *i.e.* the intact fetal membrane comprising the amnion and chorion together (n = 7). The chorion was mechanically stripped off from the intact fetal membrane to study the permeability across the amnion (n = 7) and the chorion (n = 7) separately. The experiments were conducted in dark to avoid quenching of fluorescence. Individual membranes were used to determine which membrane acts as a rate limiting barrier for the permeability of molecules based on the size. Usually the permeability of a molecule directly reflects the interactions of the molecules with the tissue and physiological properties of the tissue. The G₄-PAMAM-GABA-NH-FITC (**1**) used for transport and permeability study is hereafter referred to as dendrimer (**1**) and the unconjugated or free FITC is referred as FITC.

PAMAM dendrimers are nanosized macromolecules and their size increases from 1.1-12.4 nm as they proliferate from generations 1-10 [18]. The Alexa and FITC labeled G₄-PAMAM dendrimers (**1**, **2**) synthesized in the present study have a size of 5.6 and 5.4 nm respectively, as seen from our particle size analysis by DLS. In case of the biological compartments, the epithelium acts as a general barrier for the entry of nanosized materials into the body. The paracellular transport of nanomaterials across the epithelium is prevented by the presence of tight junctions and adherens which have a small gap < 2nm [40]. So far there has been little or no information on the transmembrane transport of G₄-PAMAM dendrimers across the human chorioamniotic membrane. In the past, carboxyfluorescein encapsulated liposomes were used to study transplacental transport [41-43] and fluorescein has been used to study transplacental transport *in vitro* using BeWo (chorionic) cell line [44]. Carboxyfluorescein does not bind to the tissue proteins, it is inert and does not undergo biotransformation and its molecular weight is similar to the commonly used therapeutic agents therefore it is considered as suitable marker for transplacental transfer [43]. Literature shows that fluorescein is established marker for transplacental transfer, hence we chose to use the fluorophore (FITC and Alexa) tagged G₄-PAMAM dendrimers in the present study.

As compared to the larger G₄-PAMAM dendrimer molecule (**1**), the small FITC molecule showed a rapid transport across all the three membranes (chorioamnion, amnion and chorion,

respectively) in first few hours (in 2-3 h) as seen from Figs. 3-5. The transport of FITC was fastest across the amnion and a near complete transport (49 %)(concentration equilibration) of FITC on the receptor side seemed to occur in 2 h (Fig. 4B). About 26 % of FITC was transported across the chorion in 5 h (Fig. 5B). The transport of FITC from chorioamnion was slower than that observed for amnion and chorion, and about 20 % transmembrane transport was seen in first 5 h (Fig. 3B), while a complete transport occurred after 20 h (Fig. 3A). The transport of G₄-PAMAM dendrimer (**1**) from all the three membranes across to the receptor side was negligible (< 3 %) in the initial few hours (5 h) (Figs. 3-5B). The transport of dendrimer (**1**) did not seem to change with respect to concentration (3 and 0.6 mg/mL) in first 5 h and was significantly low when compared to FITC. The dendrimer (**1**) transport for lower concentration (0.6 mg/mL) increased from ≤ 3 % at 5 h to 8.3 % in 20 h for chorioamnion, while for amnion it increased from ≤ 3 % at 5 h to 22 % in 20 h and for chorion in increased from 3% in 5h to 10 % in 20 h. The transport of dendrimer was slowest from chorioamnion followed by chorion and was relatively faster in amnion. To mimic the *in vivo* conditions the transport across chorioamnion is relevant. The transmembrane transport of the dendrimer (**1**) seemed to increase slightly as time progressed (24-30 h) but substantial amount of dendrimer was not found to transport when compared to FITC alone across all the three membranes as seen from Figs. 3-5A. Previously, an inverse relation with the molecular weight and the transport across the BeWo (choriocarcinoma) cell line was observed for various markers such as fluorescein, sucrose, dextrans and several amino acids of varying molecular weights[44,45]. The molecular sieving of the BeWo monolayers seemed to restrict the transport of peptides > 1033 Da and the paracellular route was major pathway for transport [45]. Our results for the G₄-PAMAM dendrimer (**1**) seem to be in agreement with those reported.

The solute membrane partition coefficient is another parameter that affects the transport across the biomembrane. The two possible pathways for the solutes to cross the fetal membrane barriers are (a) transcellular route and (b) water filled trans-trophoblastic channels. The hydrophilic molecules are mostly transported thorough the water filled channels with the exception of very few hydrophilic solutes which show transcellular transport across the human placenta [46]. The Log P values for the G₄-PAMAM dendrimers are negative indicative of its hydrophilic nature [47], therefore the transcellular mechanism of transport seems unlikely and the major transport mechanism for these molecules could be through the water filled transmembrane channels or pores. The histological evaluation was carried out to further evaluate the mechanism of transport and biodistribution discussed in subsequent sections. The overall results show that the dendrimer (**1**) in size range 5-6 nm do not cross the chorioamnion appreciably (<3%) in first 5 h. This, combined with the fact that dendrimers biodistribute relatively rapidly (with ~ 2-3 hours), suggest that dendrimers could be candidates for selective topical delivery to the mother without affecting the fetus.

3.4. Permeation of G₄-PAMAM dendrimer (**1**) and FITC

The transport of molecules across the membranes occurs as a result of passive diffusion or active transport [36]. The passive diffusion differs from the active process such that the passive diffusion of the compound through the cell membrane is dependant on the concentration gradient with a constant permeability coefficient. Previously, it has been shown that the quantity of D-arabinose or carbohydrate transferred across 1cm² of human chorion per unit gradient per unit time can be given by [48].

$$\frac{D}{\Delta x} = \frac{P}{A}$$

Where, *D* is Diffusion coefficient, Δx is the thickness of the tissue studied, *P* is the permeability constant and *A* is the area. When the permeability coefficient is known it's often used to

calculate the other unknown parameters such as diffusion coefficient (D) or partition coefficients (k) or the membrane thickness[49].

In the current study, the influence of dendrimer (**1**) size vs the small of molecule (FITC) on permeability through the fetal membranes was evaluated. As per the Fick's law of diffusion, the permeability of the solute can be given by the equation [50-52]

$$\frac{P}{\delta} = \frac{-V}{2At} \ln \frac{AC_t}{C_0}$$

where C_t is the solute concentration in the receptor cell; C_0 is the initial solute concentration in the donor cell; V is the volume of each half cell; A is the effective permeation area; P is the permeability coefficient; t is the time; and δ is the thickness of the membrane. The above equation can be rewritten as

$$\ln \left(1 - 2 \frac{C_t}{C_0} \right) = \frac{-2A}{V} Pt$$

To determine the permeability coefficient, P , a plot of $-V/2A \ln (1 - 2C_t/C_0)$ against t was constructed and linear fitting was performed. The slope of the linear portion of the graph yields a permeability coefficient. The thickness of the chorioamnion, chorion and amnion was 0.22 mm, 0.16 mm and 0.05 mm respectively ($n = 7$), as measured with the help of Mitutoyo Super Caliper. Table 1 shows the permeability coefficients for G₄-PAMAM-dendrimer (**1**) and free FITC through the different membranes. The Figs. 6A-C and Fig. 7 show the plots used for calculation of the permeability and the correlation in all the cases ranged from 0.96 to 0.99.

The permeability of FITC (Mw = 389 Da) was found to be 1.32×10^{-6} ($r^2 = 0.97$) and 2.26×10^{-6} cm²/s ($r^2 = 0.99$) for the chorion and amnion respectively. Previously, the *in vitro* permeability of cell free amnion was reported to be 1.5×10^{-6} cm²/s for D-glucose and 2-aminoisobutyrate[53]. Further, the *in vitro* permeability across chorion for meperidine (Mw = 247.33 Da) and diazepam (Mw = 284.7 Da) was reported to be 5.26×10^{-6} and 4.51×10^{-6} cm²/s respectively. Our results for the FITC seem to be within the range to those reported comparing the molecular weights of these compounds to FITC. The permeability of FITC from chorioamnion was found to be 7.93×10^{-7} cm²/s. These results show that amnion is more permeable to FITC than the chorion. The permeability of fetal membranes in rhesus monkey is similar to that of humans and the chorion and chorioamnion in the rhesus monkey were found to be less permeable than the amnion [48]. Further, previous reports arranged the permeability for water, sodium ions, urea, D-arabinose and sucrose in the order amnion > chorion = chorioamnion [54-57]. Our results for free FITC seem to be in agreement with those reported previously.

The permeability of small molecule FITC is 100 folds higher from chorion and amnion alone when compared to the permeability of G₄-PAMAM-dendrimer (**1**). When permeability across chorioamnion (intact membrane) was compared, FITC was found to be 9-fold more permeable than the dendrimer (**1**) (Table 1). We found that the permeability of the compounds was inversely proportional to their molecular weights. The permeability of dendrimer (**1**) in the amnion was concentration dependant with a value of 1.86×10^{-8} cm²/s ($r^2 = 0.98$) for low concentration and 2.08×10^{-7} cm²/s ($r^2 = 0.97$) for the higher concentration (Table 1). While in case of the chorioamnion the lower concentration (0.6 mg/mL) showed a slightly higher permeability (7.5×10^{-8} cm²/s) ($r^2 = 0.97$) than that exhibited by the higher (3 mg/mL) concentration (5.8×10^{-8} cm²/s) ($r^2 = 0.98$). On the other hand, the chorion alone did not show

a concentration dependant permeability where both the high and low concentrations showed a permeability coefficient of $2.94 \times 10^{-8} \text{ cm}^2/\text{s}$ ($r^2 = 0.96$ and 0.97 respectively) (Fig. 6C)). In the present study, the amnion and the chorioamnion were able to differentiate between the high and low concentrations of the dendrimer (**1**) unlike the chorion (Fig. 6A-B). Previous reports have shown that the human amnion has better ability to differentiate between different cations than the chorion, and also the amnion has better differentiating ability towards the transport of small non electrolytes and water than the chorion [50,53,54,58]. The order of conductance of cations by different layers was reported to be amnion = chorioamnion > chorion [54]. These differences are attributed to the larger intercellular sites in chorion when compared to amnion and hence the chorion cannot differentiate between the cations [54]. The entrapped water in the amnion forms an unstirred water layer which itself acts as an effective diffusional barrier to transport of molecules in addition to the amniotic membrane structure [53] and the human amnion cell layer is a more effective diffusion barrier than chorion [50,58].

The molecular weight of the G₄-PAMAM-O-GABA-NH-FITC (**1**) is approximately 40 times higher (~ 16 kDa) than the molecular weight of FITC (389 Da) and based on the dendrimer size, its transport is hindered across the membranes. The fetal membranes allow the passage of small molecules (< 600 Da) like sodium and glucose by simple diffusion but do not readily permit the passage of substances of molecular weight > 1000 Da [59,60]. The amnion and the chorioamnion, behave physicochemically as porous and partially semipermeable membranes and their cell junctions made of desmosomes, gap junctions and occasional tight junctions offering resistance for paracellular transport [59-62]. The human chorion is sieve-like membrane with large water filled extracellular channels and also the intercellular spaces [59, 60]. The transfer by paracellular pathway is more important than the transcellular pathway in the fetal membranes. The paracellular transfer is dependant on the different pore sizes and the trophoblast in chorion region has limited number of dilated branching wide openings with a diameter of 15-25 nm which regulate the overall permeability. While the non dilated channels in chorion provide transport for the smaller substances having an effective molecular radius under 2 nm, the clefts at the intercellular junctions further have few tight regions of 4.1 nm in diameter restricting the passage of large molecules [37]. The size of G₄-PAMAM-Alexa (**2**) and G₄-PAMAM-FITC (**1**) was found to be 5.6 nm and 5.4 nm respectively, and hence their passage could occur through the limited dilated openings in chorion.

We observed a linear relationship between the rate of transport and the concentration of dendrimer (**1**) till 5 h which shows that the transfer (< 3%) occurs by passive diffusion for all the three membranes in this time frame. This observation was from both the permeability and transmembrane transport plots till 5 h (Figs. 3-5B and 6A-C). At later time points (5 to 30 h), as seen from the plots of transmembrane transport (Figs. 1-3A), the dendrimer (**1**) with higher (3 mg/mL) concentration showed a lower transport as compared to the lower concentration (0.6 mg/mL). This suggests that the major pathway for transport in initial phase (upto 5-6 h) is passive diffusion but at later times a saturable process for the transport of higher concentration is likely, suggesting an additional pathway for transport across the membrane. Valproic acid uptake (and transport) by the trophoblast cells is energy dependant (carrier mediated) and was saturable at higher concentration [63]. Further, despite similar molecular weights, the transport of lipophilic compound was substantially higher than the hydrophilic compound [64]. In this study, varying the donor concentration of dendrimer (**1**) did not lead to a significant change in the permeability coefficient in the chorioamnion and the chorion (Table 1). However, the permeability through the amnion alone was found to differ with change in concentration of the dendrimer. These findings suggest that transmembrane transport of dendrimers occurs by paracellular and energy dependant pathways.

The previous reports on transplacental and transmembrane transport of macromolecules like thyrotropin stimulating hormone (TSH), with molecular weight 28 kDa using a dual chamber

was found to be negligible across the placenta and fetal membranes[64,65]. Our finding for dendrimers (1) are similar those reported. The results of present study show that fetal membranes exhibit barrier properties for transmembrane transport based on molecular weight. These results are consistent with those reported in past[60,64,65]. The experimental observation and inferential evidence suggests that if the drugs are conjugated to the dendrimers or other polymers of large molecular weights, then their transport across the fetal membranes will be restricted due to the larger size in conjugated form and these agents could be used for the selective topical delivery in pregnant women without affecting the fetus. It must be pointed out the present measurements of diffusion from a high concentration water solution across the chorioamniotic membrane in a side-by-side chamber would overestimate the transport, when compared to a topical application, where volume of the body fluids will be present at relatively lower levels.

3.5. Biodistribution of dendrimer in the chorioamniotic membrane

Confocal microscopy was used for histological visualization of the transport and biodistribution of dendrimer (2) (G4-PAMAM-GABA-NH-Alexa) across the chorioamniotic membrane. Fig. 8A shows the general morphology of the human chorioamniotic membrane. The Fig. 8B shows the control membrane (without the treatment with dendrimer (2)) and with negative controls rabbit isotype and mouse isotype replacing the primary antibodies showing the nuclei stained blue with DAPI. To identify the different cells and regions in the chorioamniotic membranes they were stained with cytokeratin and vimentin positive. The transport of the dendrimer (2) across the chorioamniotic membrane as a function of time was investigated and the histology data is shown in Fig. 9. The nuclei for all cells are stained blue (by DAPI), the trophoblast cells in the chorion region are stained cytokeratin positive (red) and the stromal cells in the decidua are stained vimentin positive (magenta). The progressive advancement of the dendrimer (2) front across the membrane with respect to the time (30 min to 4 h) can be visualized from Fig. 9. The dendrimer (2) is mostly confined to the chorionic regions in the membrane as seen from the differential staining for the amnion and chorionic regions (Fig. 9). At early time points, 30 min to 2 h (Fig. 9 top panel) the dendrimer (2) is mostly seen in the decidual region and not much has traversed into the trophoblast region (stained red). While at 2.5 to 3.5 h time points the dendrimer (2) transport has progressed slightly further and sparsely the dendrimer can be visualized in the trophoblast cells in the chorionic region, though most of the dendrimer seems retained in the decidual region (Fig. 9, middle panel). After 4 h the dendrimer (2) seems to have traversed into the trophoblast regions as seen from the image (Fig. 9, bottom panel extreme left).

It is interesting to note that with the passage of time (30 min to 4 h) the dendrimer (2) progresses gradually across the decidua into the trophoblast region, however a corresponding increase of the dendrimer (2) transport across the chorion mesoderm, spongy layer, reticular mesh of fibroblast layer, amniotic mesoderm or amniotic epithelium is not observed from the histological evaluation (Fig. 9). In general, the histology of membranes shows that the dendrimer (2) is not seen in the chorioamniotic mesoderm and amniotic epithelium for the entire time frame (30 min-4 h). It is reported that the human amnion epithelial cells express the multidrug resistant associated proteins (MRPs) which are responsible for preventing the accumulation of xenobiotics and contribute for their efflux out of the amnion cells [66]. A similar mechanism was speculated for the negligible transport of alkaline phosphatase (180 kDa) across the amniotic epithelial cells, while the small molecules (< 600 Da) were reported to be largely transported by paracellular pathways [66]. Our transport experiments showed ≤ 3 % transfer of dendrimer from the chorioamnion upto 5 h. It appears from the immunofluorescence images that whatever dendrimer traverses across chorionic trophoblast region is also transported across the amnion without being retained by the amnion cell layer, while the dendrimer is mostly accumulated and retained by the chorionic trophoblast region.

To further evaluate if the dendrimers were taken up by the cells in the chorionic region the histology of membranes was evaluated under higher magnification (63x). The colocalization images (Fig. 10A-B) with either cytokeratin or vimentin show the internalization of dendrimer (2) in both cytokeratin positive trophoblast cells and vimentin positive stromal cells. The colocalization of the dendrimer (2) is seen in the nuclei of the trophoblast cells in chorion (Fig. 10B) and the nuclei and cytoplasm of stromal cells in decidua (Fig. 10A). Further, the image (Fig. 10A) shows that the dendrimer (2) surrounds these stromal cells suggesting that both paracellular and transcellular mechanisms could be responsible for transport, though passive diffusion seems to be dominant and only a small fraction of the dendrimer (2) might be internalized in the cells. A similar observation was seen for the trophoblast cells where the dendrimer is largely found in interstitial spaces as compared to that being taken up in nuclei (Fig. 10B). Internalization of dendrimers into the lysosome and cytoplasm by endocytosis in A549 lung epithelial cells has been previously reported [67]. Further, colocalization of dendrimers in cytoplasm and nucleus of HeLa and cancer cells is known [68,69]. Also transport of dendrimers by paracellular and transcellular pathway for Caco-2 cell line and microglial cell line [70-73] is reported in the past. Based on our observations and the evidence from past literature showing internalization of dendrimers in several cells, it appears that the dendrimer is indeed internalized in some of the trophoblast and stromal cells in fetal membranes.

Cellular permeation pathways exist in human fetal membranes and they are capable of differentiating between different molecular species [58]. Our transport data showed that the higher concentration of the dendrimer (3 mg/mL) at later time points (20-30 h) did not show the proportionately higher transport across the membranes. This suggests that the concentration gradient was not the only driving force for the transport and there could be a possibility of dendrimer being retained in the cells. It is possible that the cells are saturated at higher concentration of dendrimer and hence the correspondingly higher transport at this concentration was not observed. Our histology data for later time point 4h showed internalization of dendrimer (2) in most stromal cells (Fig. S3, Supporting information). A saturable phenomenon for transport was observed for higher concentration of valproic acid in trophoblast cells [63]. The transtrophoblast transfer of D-glucose and 2-aminoisobutyrate showed both saturable and non-saturable pathways and accumulation in trophoblast cells. These previous results collectively with the transport data and histological evaluation of immunofluorescent images suggest that some dendrimer (2) could be retained intracellularly in the layers of the chorioamnion membrane. There are reports indicating that certain types of particles are accumulated in the placental membrane cells rather than crossing the barriers after extended time periods [37]. The gold nanoparticles 10-30 nm were internalized in the placental cells (trophoblast cells) and traceable amounts were not transported to the fetal side in 6 h [37]. Also, the energy dependant pathway for internalization of the small liposomes (70 nm) probably by endocytosis in the placental tissues was reported. Some amount of the liposomes (70 nm) was transported by endocytosis to the fetal side. The large multilamellar liposomes (300 nm) were minimally internalized and the anionic and neutral liposomes were preferentially internalized over the cationic liposomes[43].

The most significant observation from the present study is that the G₄-PAMAM dendrimers do not cross the intact human fetal membrane significantly (<3%) in 5 h, and cross in relatively small amounts (~10%) over extended time periods up to 20 h. The dendrimer is mostly seen retained in chorionic regions. Our results show that when compared to the smaller molecules (*e.g.* free FITC) which show rapid transport across the chorioamnion (intact membrane) the G₄-PAMAM dendrimers showed relatively negligible transport. The strength of this study is that it was conducted on the fetal membranes of women who underwent cesarean-section delivery and had intact fetal membranes. This investigation of transmembrane transport of dendrimer from intact fetal membranes is more relevant to correlate with the transport of dendrimers from formulations applied to pregnant women topically on the vaginal mucosa.

The polylysine based dendrimers are used as topical microbicidal agents to treat genital herpes and the vaginal gels based formulations are currently under human clinical trials. Recently, the PAMAM dendrimers were reported to exhibit antimicrobial activity [21]. The present study indicates that these dendrimers could be used as topical antimicrobial agents or as a component in any intravaginal dosage form (e.g. vaginal tablet, solution or gel) and possibly be used in pregnant women without rapidly crossing into the fetus. These are the preliminary results and further extensive investigations are under way.

4. Conclusions

Selective treatment of the pregnant women without affecting the fetus is always desired which probes the search for effective drug delivery approaches. The transmembrane transport for G₄-PAMAM dendrimer and FITC was measured across intact human chorioamnion (fetal) membrane and through the stripped amnion and chorion membrane individually. Indeed, the G₄-PAMAM dendrimers (Mw ~16 kDa) tagged with FITC showed significantly slower rate of transport across the fetal (chorioamniotic) membranes when compared to the transplacental marker free FITC (Mw ~389 Da). The dendrimer transport was less than $\leq 3\%$ from all the membranes upto 5 h and increased slightly in 20h, with about 8.3% for chorioamnion (intact membrane), 22 % for amnion and 10.5 % for chorion, respectively. The transport of FITC was fastest across the amnion with almost complete FITC seen on the receptor side in 2 h (49 %), about 26 % in 5 h from chorion and 20 % across chorioamnion in 5 h, respectively. The biodistribution study showed that the dendrimer is mostly retained in the decidual stromal cells in 30 min to 2 h. With progression in time the dendrimer traverses upto the chorionic trophoblast cells (2.5 to 4 h). To some extent, the dendrimer is internalized in nuclei of trophoblast cells and nuclei and cytoplasm of stromal cells. Largely, the dendrimer is seen in the interstitial regions of stromal and trophoblast cells indicating the passive diffusion as major transport route. The results suggest that dendrimers could be used as topical antimicrobial agents or as components of intravaginal dosage forms for selective treatment of pregnant women without affecting the fetus. The overall findings further suggest that entry of drugs conjugated to macromolecules would be restricted across the human fetal membrane when administered topically by intravaginal route.

Supplementary Material

Refer to Web version on PubMed Central for supplementary material.

Acknowledgments

This study was supported by the Intramural Research Program of the National Institute of Child Health and Human Development, NIH, DHHS.

References

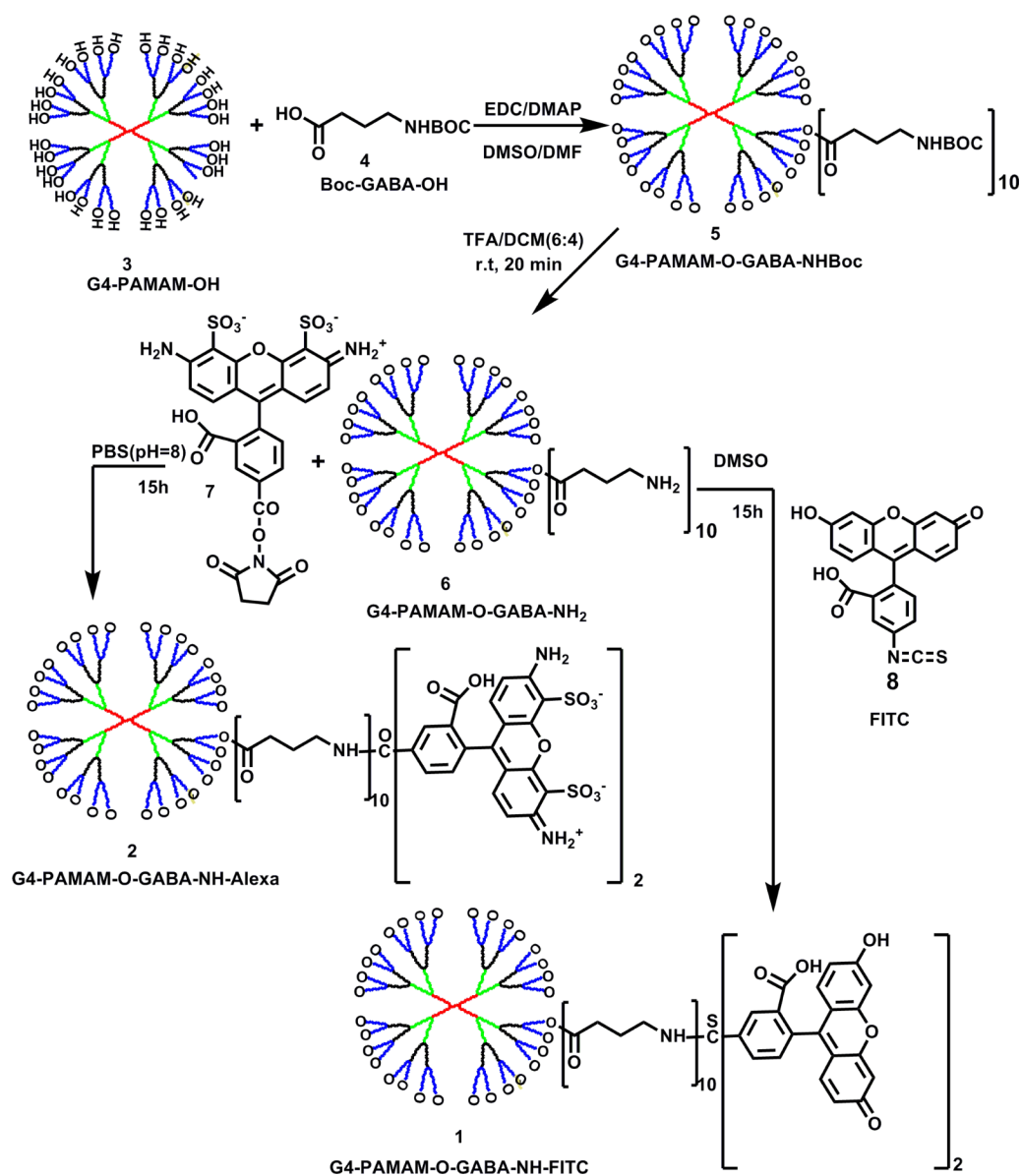
1. Audus KL. Controlling drug delivery across the placenta. *Eur J Pharm Sci* 1999;8(3):161–165. [PubMed: 10379038]
2. Nicolle LE. Use of Antimicrobials during Pregnancy. *Can Fam Physician* 1987;33:1247–1251.
3. Sastry BV. Techniques to study human placental transport. *Adv Drug Deliv Rev* 1999;38(1):17–39. [PubMed: 10837744]
4. Ndesendo VM, Pillay V, Choonara YE, Buchmann E, Bayever DN, Meyer LC. A review of current intravaginal drug delivery approaches employed for the prophylaxis of HIV/AIDS and prevention of sexually transmitted infections. *AAPS PharmSciTech* 2008;9(2):505–520. [PubMed: 18431651]
5. Chaim W, Mazor M, Leiberman JR. The relationship between bacterial vaginosis and preterm birth. A review. *Arch Gynecol Obstet* 1997;259:51–58. [PubMed: 9059744]

6. Soong D, Einarson A. Vaginal yeast infections during pregnancy. *Can Fam Physician* 2009;55:255–256. [PubMed: 19282531]
7. Ugwumadu A. Role of antibiotic therapy for bacterial vaginosis and intermediate flora in pregnancy. *Best Pract Res Clin Obstet Gynaecol* 2007;21(3):391–402. [PubMed: 17512255]
8. Romero R, Chaiworapongsa T, Espinoza J. Micronutrients and intrauterine infection, preterm birth and the fetal inflammatory response syndrome. *J Nutr* 2003;1668S–1673S. [PubMed: 12730483]
9. Stone A. Microbicides: a new approach to preventing HIV and other sexually transmitted infections. *Nat Rev Drug Discov* 2002;1(12):977–985. [PubMed: 12461519]
10. Lebreton S, Newcombe N, Bradley M. Antibacterial single-bead screening. *Tetrahedron* 2003;59:10213–10222.
11. Balogh L, Swanson DR, Tomalia DA, Hagnauer GL, McManus AT. Dendrimer-Silver complexes and nanocomposites as antimicrobial agents. *Nano Lett* 2001;1:18–21.
12. Cheng Y, Qu H, Ma M, Xu Z, Xu P, Fang Y, et al. An in vitro study Polyamidoamine (PAMAM) dendrimers as biocompatible carriers of quinolone antimicrobials. *Eur J Med Chem* 2007;42:1032–1038. [PubMed: 17336426]
13. Devarakonda B, Li N, deVilliers MM. Effect of Polyamidoamine (PAMAM) dendrimers on the in vitro release of water-insoluble nifedipine from aqueous gels. *AAPS PharmSciTech* 2005;6(3):504–512.
14. Unal B, Hedden RC. pH-dependent swelling of hydrogels containing highly branched polyamine macromonomers. *Polymer* 2009;50:905–912.
15. Wu X, Huang SW, Zhang JT, Zhuo RX. Preparation and characterization of novel physically cross-linked hydrogels composed of poly(vinyl alcohol) and amine-terminated polyamidoamine dendrimer. *Macromol Biosci* 2004;4:71–75. [PubMed: 15468196]
16. Patton DL, Cosgrove Sweeney YT, McCarthy TD, Hillier SL. Preclinical safety and efficacy assessments of dendrimer-based (SPL7013) microbicide gel formulations in a nonhuman primate model. *Antimicrob Agents Chemother* 2006;50(5):1696–1700. [PubMed: 16641437]
17. Mumper RJ, Bell MA, Worthen DR, Cone RA, Lewis GR, Moench TR. Formulating a sulfonated anti-viral dendrimer in a vaginal microbicidal gel having dual mechanisms of action. *Drug Dev Ind Pharm* 2009;35(5):515–524. [PubMed: 19040181]
18. Svenson S, Tomalia DA. Dendrimers in biomedical applications-reflections on the field. *Adv Drug Deliv Rev* 2005;57(15):2106–2129. [PubMed: 16305813]
19. Bernstein D, Stanberry LR, Sacks S, Ayisi NK, Gong YH, Ireland J, et al. Evaluations of unformulated and formulated dendrimer-based microbicide candidates in mouse and guinea pig models of genital herpes. *Antimicrob Agents Chemother* 2003;47(12):3784–3788. [PubMed: 14638483]
20. <http://clinicaltrials.gov/ct2/results?term=SPL7013>
21. Calabretta MK, Kumar A, McDermott AM, Cai C. Antibacterial activities of Poly(amidoamine) dendrimers terminated with amino and poly(ethylene glycol) groups. *Biomacromolecules* 2007;8:1807–1811. [PubMed: 17511499]
22. Tulu M, Aghatabay NM, Senel M, Dizman C, Parali T, Dulger B. Synthesis, characterization and antimicrobial activity of water soluble dendritic macromolecules. *Eur J Med Chem* 2009;44:1093–1099. [PubMed: 18657884]
23. Ortega P, Copa-Patino JL, Munoz-Fernandez MA, Soliveri J, Gomez R, Mata FJ. Amine and ammonium functionalization of chloromethylsilane-ended dendrimers: Antimicrobial activity studies. *Org Biomol Chem* 2008;6:3264–3269. [PubMed: 18802631]
24. Chen CZ, Cooper SL. Interactions between dendrimer biocides and bacterial membranes. *Biomaterials* 2002;23:3359–3368. [PubMed: 12099278]
25. Chen CZ, Beck-Tan NC, Dhurjati P, Van Dyk TK, LaRossa RA, Cooper SL. Quaternary ammonium functionalized Poly(propylene imine) dendrimers as effective antimicrobials: structure-activity studies. *Biomacromolecules* 2000;1:473–480. [PubMed: 11710139]
26. Cloninger MJ. Biological applications of dendrimers. *Curr Opin Chem Biol* 2002;6:742–748. [PubMed: 12470726]
27. Rosenstein IJ, Morgan DJ, Lamont RF, Sheehan M, Dor CJ, Hay PE, et al. Effect of intravaginal clindamycin cream on pregnancy outcome and on abnormal vaginal microbial flora of pregnant women. *Infectious Diseases in Obstetrics and Gynecology* 2000;8:158–165. [PubMed: 10968599]

28. Drake S, Taylor S, Brown D, Pillay D. Improving the care of patients with genital herpes. *BMJ* 2000;321(9):619–623. [PubMed: 10977846]
29. Ylikorkala O, Sjöstedt E, Järvinen PA, Tikkanen R, Raines T. Trimethoprim-sulfonamide combination administered orally and intravaginally in the first trimester of pregnancy: its absorption into serum and transfer to amniotic fluid. *Acta Obstetrica et Gynecologica Scandinavica* 1973;52:229–234. [PubMed: 4743777]
30. <http://www.drugs.com/pro/terconazole.html> and <http://dailymed.nlm.nih.gov/dailymed/drugInfo.cfm?id=8383>
31. Sosnik A, Chiappetta DA, Carcaboso ÁM. Drug delivery systems in HIV pharmacotherapy: What has been done and the challenges standing ahead. *J Control Rel* 2009;138:2–15.
32. <http://clinicaltrials.gov/ct2/show/NCT00540605>
33. Cheng Y, Man N, Xu T, Fu R, Wang X, Wang X, et al. Transdermal delivery of nonsteroidal anti-inflammatory drugs mediated by polyamidoamine (PAMAM) dendrimers. *J Pharm Sci* 2007;96(3):595–602. [PubMed: 17094130]
34. Chauhan AS, Sridevi S, Chalasani KB, Jain AK, Jain SK, Jain NK, et al. Dendrimer-mediated transdermal delivery: enhanced bioavailability of indomethacin. *J Control Release* 2003;90(3):335–343. [PubMed: 12880700]
35. Kim SS, Romero R, Kim JS, Abbas A, Espinoza J, Kusanovic JP, et al. Coexpression of myofibroblast and macrophage markers: novel evidence for an in vivo plasticity of chorioamniotic mesodermal cells of the human placenta. *Lab Invest* 2008;88:365–374. [PubMed: 18227805]
36. Zheng Y, Qiu Y, Lu MF, Hoffman D, Reiland TL. Permeability and absorption of leuprolide from various intestinal regions in rabbits and rats. *Int J Pharm* 1999;185:83–92. [PubMed: 10425368]
37. Myllynen P, Loughran MJ, Howard CV, Sormunen R, Walsh AA, Vähäkangas KH. Kinetics of gold nanoparticles in the human placenta. *Reprod Toxicol* 2008;26:130–137. [PubMed: 18638543]
38. Miller R, Mace K, Polliotti B, DeRita R, Hall W, Treacy G. Marginal transfer of ReoPro (Abciximab) compared with immunoglobulin G (F105), inulin and water in the perfused human placenta in vitro. *Placenta* 2003;24:727–738. [PubMed: 12852863]
39. Kurtoglu YE, Mishra MK, Kannan S, Kannan RM. Drug release characteristics of PAMAM dendrimer–drug conjugates with different linkers. *Int J Pharm* 2009;384:189–194. [PubMed: 19825406]
40. Saunders M. Transplacental transport of nanomaterials. *Adv Rev* 2009;1:671–684.
41. Bajoria R, Contractor SF. Effect of size of liposomes on transplacental transfer of carboxyfluorescein across the perfused human term placenta. *J Pharm Pharmacol* 1997a;49:675–681. [PubMed: 9255710]
42. Bajoria R, Contractor SF. Effect of surface charge of small unilamellar liposomes on uptake and placental transfer of carboxyfluorescein. *Pediatr Res* 1997b;42:520–527. [PubMed: 9380447]
43. Bajoria R, Sooranna SR. Liposome as a drug carrier system: Prospects for safer prescribing during pregnancy. *Trophoblast Research* 1998;12:265–287.
44. Liu F, Soares MJ, Kenneth LA. Permeability properties of monolayers of the human trophoblast cell line BeWo. *Am J Physiol Cell Physiol* 1997;273:1596–1604.
45. Ampasavate C, Chandorkar GA, Velde DGV, Stobaugh JF, Audus KL. Transport and metabolism of opioid peptides across BeWo cells, an in vitro model of the placental barrier. *Int J Pharm* 2002;233:85–98. [PubMed: 11897413]
46. Powell TL, Jansson T, Illsley NP, Wennergren M, Korotkova M, Strandvik B. Composition and permeability of syncytiotrophoblast plasma membranes in pregnancies complicated by intrauterine growth restriction. *Biochimica et Biophysica Acta* 1999;1420:86–94. [PubMed: 10446293]
47. Giri J, Diallo MS, Goddard WA, Dalleska NF, Tang XFY. Partitioning of Poly(amidoamine) Dendrimers between n-Octanol and Water. *Environ Sci Technol* 2009;43:5123–5129. [PubMed: 19673317]
48. Battaglia F, Bruns PD, Behrman RE, Seeds AE, Hellegers AE. Comparison of permeability of different layers of the primate placenta to D-arabinose and urea. *Am J Physiol* 1964;2007(2):500–502. [PubMed: 14205373]
49. Poletto FS, Jäger E, Cruz L, Pohlmann AR, Guterres SS. The effect of polymeric wall on the permeability of drug-loaded nanocapsules. *Mater Sci Eng: C* 2008;28(4):472–478.

50. Beall MH, van den Wijngaard JPHM, van Gemert MJC, Ross MG. Amniotic fluid water dynamics. *Placenta* 2007;28:816–823. [PubMed: 17254633]
51. Ye Z, Rombout P, Remon JP, Vervaeke C, Van den Mooter G. Correlation between the permeability of metoprolol tartrate through plasticized isolated ethylcellulose/hydroxypropyl methylcellulose films and drug release from reservoir pellets. *Eur J Pharm Biopharm* 2007;67:485–490. [PubMed: 17383166]
52. Gholap S, Jog JP, Badiger MV. Synthesis and characterization of hydrophobically modified poly (vinyl alcohol) hydrogel membrane. *Polymer* 2004;45:5863–5873.
53. Bullen B, Bloxam DL, Ryder TA, Mobberley MA, Bax CMR. Two-sided culture of human placental trophoblast. morphology, immunocytochemistry and permeability properties. *Placenta* 1990;11:431–450. [PubMed: 1707171]
54. Bara A, Bara M. Comparative study of the human amnion, chorion and chorioamnion permeability to monovalent cations. *Eur J Obstet Gynecol Reprod Biol* 1983;16:1–7. [PubMed: 6313442]
55. Seeds AE, Schrufer JJ, Reinhardt JA, Garlid KD. Diffusion mechanisms across human placental tissue. *Gynec Invest* 1973;4:31–37. [PubMed: 4710329]
56. Moore WM, Hellegers AE, Battaglia FC. In vitro permeability of different layers of the human placenta to carbohydrates and urea. *Am J Obstet Gynecol* 1966;96(7):951–955. [PubMed: 4959176]
57. Welsch F. Human fetal membranes: investigations on membrane potentials and membrane ^{24}Na permeability in vitro and the possible involvement of acetylcholine. *Gynecol Obstet Invest* 1981;12(3):113–122. [PubMed: 7239347]
58. Hardy M, Leonard RT, Scheide JJ. Cellular permeation pathways in a leaky epithelium: the human amniochorion. *Biol Cell* 1989;60:149–153. [PubMed: 2804455]
59. Lemancewicz A, Laudanaka H, Laudanaski T, Karpiuk A, Batra S. Permeability of fetal membrane to calcium and magnesium: possible role in preterm labour. *Human Reprod* 2000;15(9):2018–2022.
60. Seeds AE. Osmosis across term human placental membranes. *Am J Physiol* 1970;219(2):551–554. [PubMed: 5464994]
61. Wang T, Schneider J. Fine structure of human chorionic membrane. *Arch Gynecol Obstet* 1983;233(3):187–198.
62. Verikouki CH, Hatzoglou CH, Gourgoulis KI, Molyvdas PA, Kallitsaris A, Messinis IE. Rapid effect of progesterone on transepithelial resistance of human fetal membranes: Evidence for non-genomic action. *Clinic Exp Pharm Physiol* 2008;35:174–179.
63. Utoguchi N, Audus KL. Carrier-mediated transport of valproic acid in BeWo cells, a human trophoblast cell line. *Int J Pharm* 2000;195:115–124. [PubMed: 10675689]
64. Bajoria R, Ryder TA, Fisk NM. Transport and metabolism of thyrotrophin-releasing hormone across the fetal membrane. *J Clin Endocrinol Metab* 1997;82(10):3399–3407. [PubMed: 9329376]
65. Bajoria R, Fisk NM. Permeability of human placenta and fetal membranes to thyrotrophin-stimulating hormone in vitro. *Pediatr Res* 1998;43(5):621–628. [PubMed: 9585008]
66. Aye IL, Paxton JW, Evseenko DA, Keelan JA. Expression, localisation and activity of ATP binding cassette (ABC) family of drug transporters in human amnion membranes. *Placenta* 2007;28(8-9): 868–877. [PubMed: 17482262]
67. Perumal OP, Inapagolla R, Kannan S, Kannan RM. The effect of surface functionality on cellular trafficking of dendrimers. *Biomaterials* 2008;29(24-25):3469–3476. [PubMed: 18501424]
68. Lee S, Nam K, Park J-S, Choi JS, Eo SK, Yoo DJ, Kang SH. Extra- and Intranuclear dynamics and distribution of modified-PAMAM polyplexes in living cells: A single-molecule analysis. *Bull Korean Chem Soc* 2008;29(8):1565–1568.
69. Patil ML, Min Zhang, Taratula O, Garbuzenko OB, He H, Minko T. Internally Cationic Polyamidoamine PAMAM-OH Dendrimers for siRNA Delivery: Effect of the Degree of Quaternization and Cancer Targeting. *Biomacromolecules* 2009;10:258–266. [PubMed: 19159248]
70. Kurtoglu YE, Navath RS, Wang B, Kannan S, Romero R, Kannan RM. Poly(amidoamine) dendrimer-drug conjugates with disulfide linkages for intracellular drug delivery. *Biomaterials* 2009;30(11): 2112–2121. [PubMed: 19171376]
71. Navath RS, Kurtoglu YE, Wang B, Kannan S, Romero R, Kannan RM. Dendrimer-drug conjugates for tailored intracellular drug release based on glutathione levels. *Bioconjug Chem* 2008;19(12): 2446–2455. [PubMed: 19053299]

72. Wang B, Navath RS, Romero R, Kannan S, Kannan RM. Anti-inflammatory and anti-oxidant activity of anionic dendrimer-N-acetyl cysteine conjugates in activated microglial cells. *Int J Pharm* 2009;377(1-2):159–168. [PubMed: 19463931]
73. Kitchens K, El-Sayed MEH, Ghandehari H. Transepithelial and endothelial transport of poly (amidoamine) dendrimers. *Adv Drug Del Rev* 2005;57:2163–2176.



Scheme 1.

The schematic representation for the synthesis of fluorescently labeled G₄-PAMAM-dendrimers; G₄-PAMAM-O-GABA-NH-FITC (1) and G₄-PAMAM-O-GABA-NH-Alexa (2).

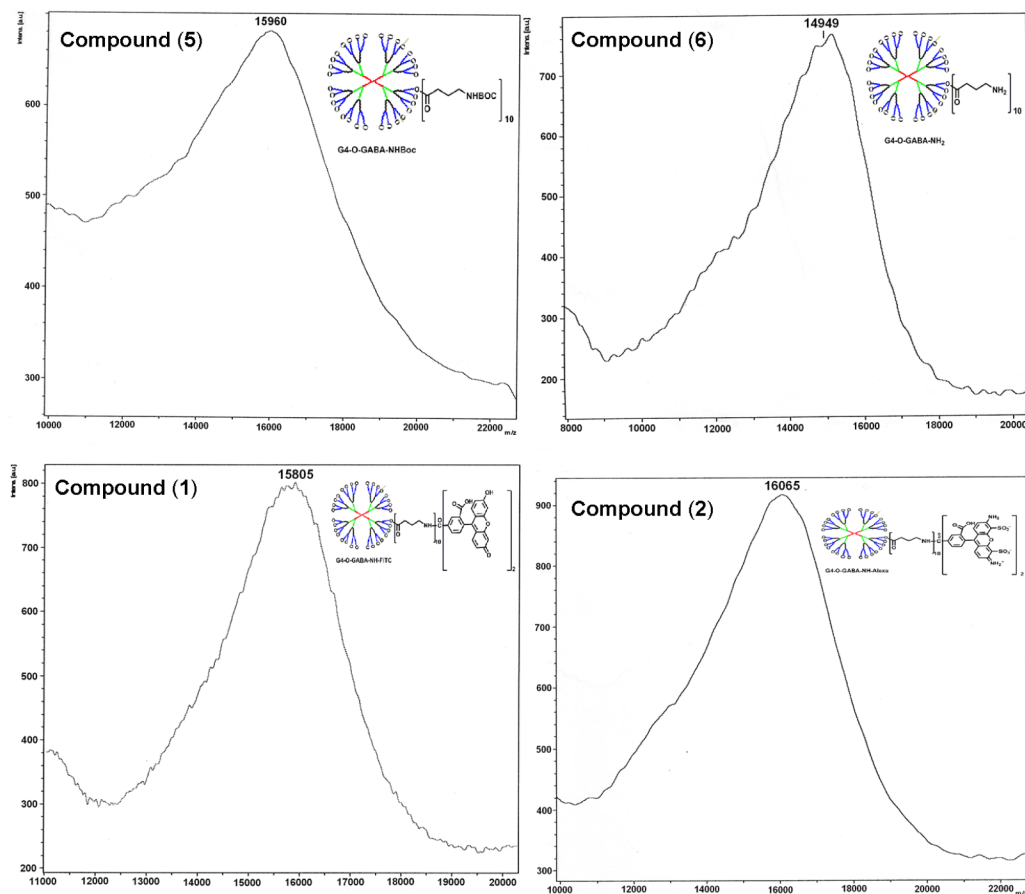


Fig. 1. MALDI TOF MS spectra for G4-PAMAM-O-GABA-Boc (**5**) (Mw = 15,960 Da), G4-PAMAM-O-GABA-NH₂ (**6**) (Mw = 14,949 Da), G4-PAMAM-O-GABA-NH-FITC (**1**) (Mw = 15,805 Da) and G4-PAMAM-O-GABA-NH-Alexa (**2**) (Mw = 16,065 Da) showing the corresponding mass.

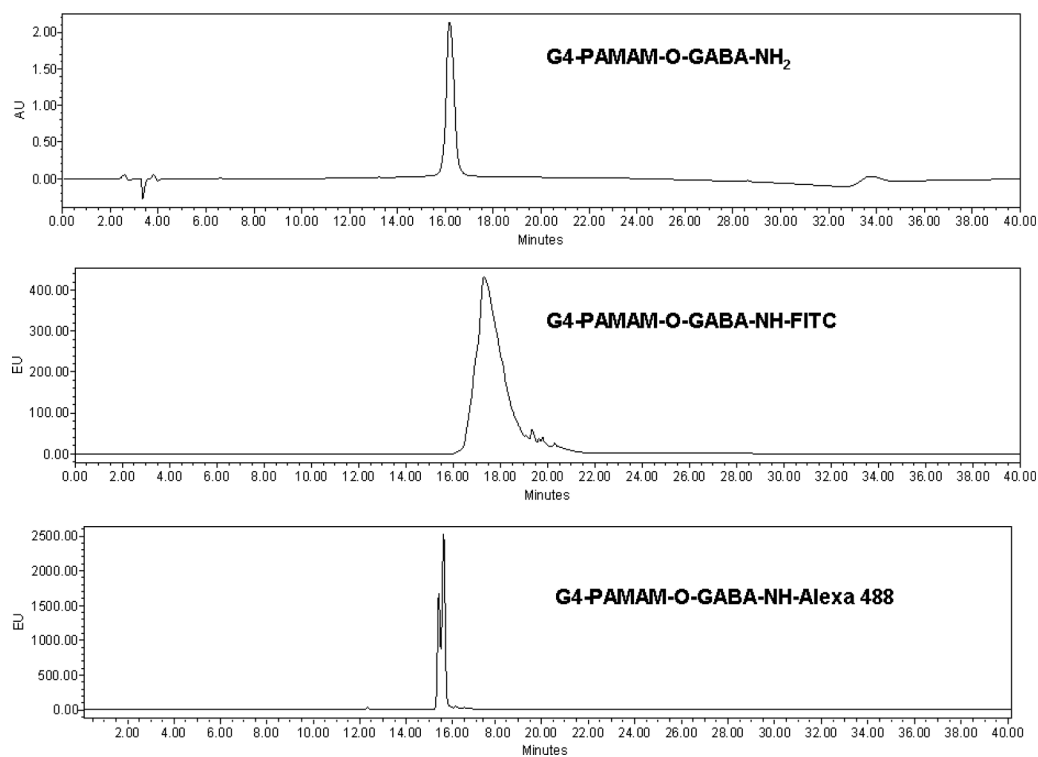


Fig. 2. HPLC chromatograms for G4-PAMAM-O-GABA-NH₂ (**6**) (UV channel), G4-PAMAM-O-GABA-NH-FITC (**1**) (Fluorescent channel) and G4-PAMAM-O-GABA-NH-Alexa 488 (**2**) (Fluorescent channel). The retention time of G4-PAMAM-O-GABA-NH₂ is 16.2 min and the FITC and Alexa tagged G4-PAMAM-O-GABA-NH₂ show a peak appearing at 17.5 and 15.5 min respectively.

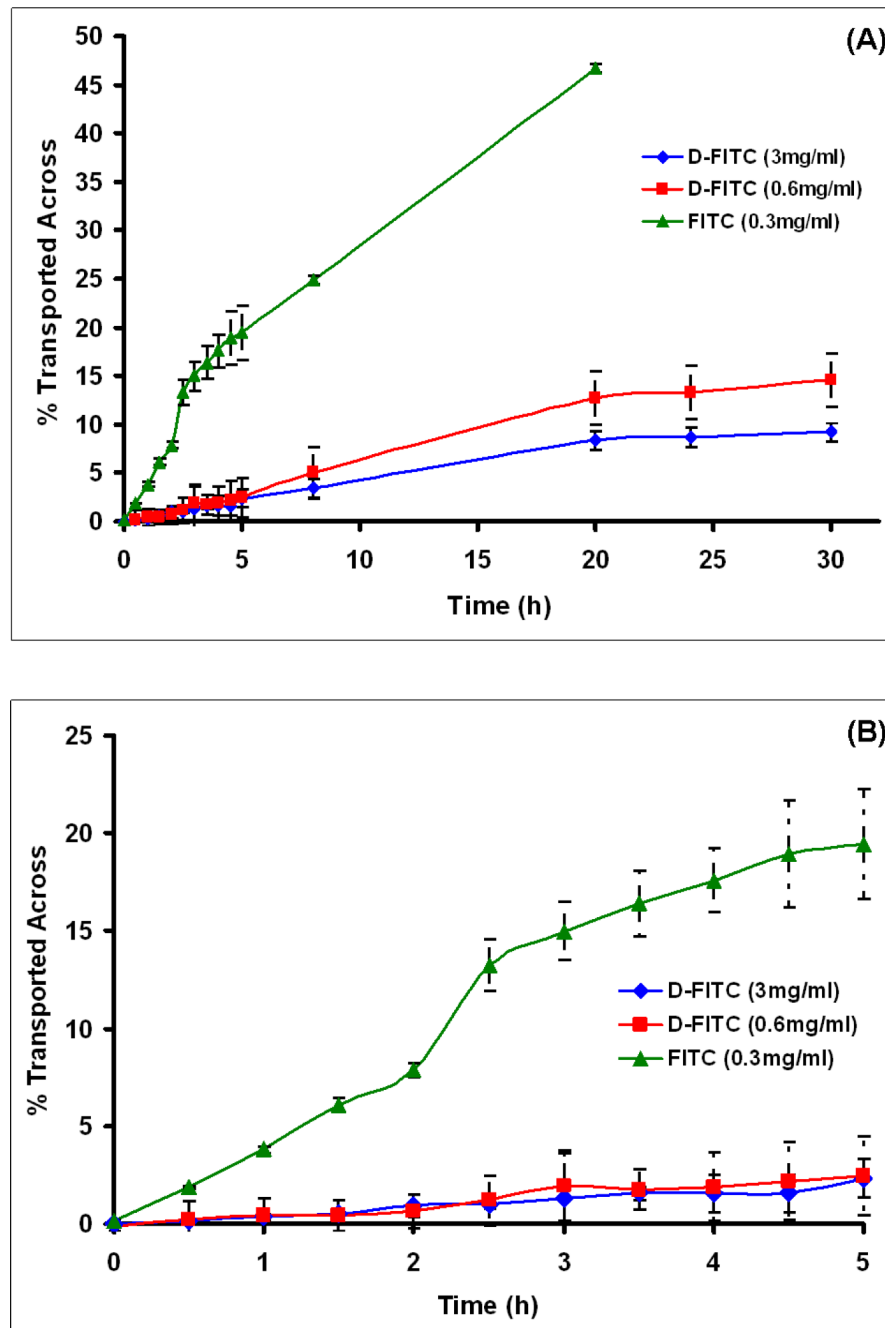


Fig. 3. (A) The transport of G_4 -PAMAM-O-GABA-NH-FITC (D-FITC) and FITC (unconjugated) across the fetal membrane comprising amnion and chorion together over 30h in the side by side diffusion chamber. (B) The FITC shows a rapid transport across the membrane in 5 h (~20%), while the dendrimers show negligible transport of $\leq 3\%$ in 5 h. The concentrations of D-FITC studied were 0.6 mg/mL and 3 mg/mL. The concentration of FITC was 0.3 mg/mL.

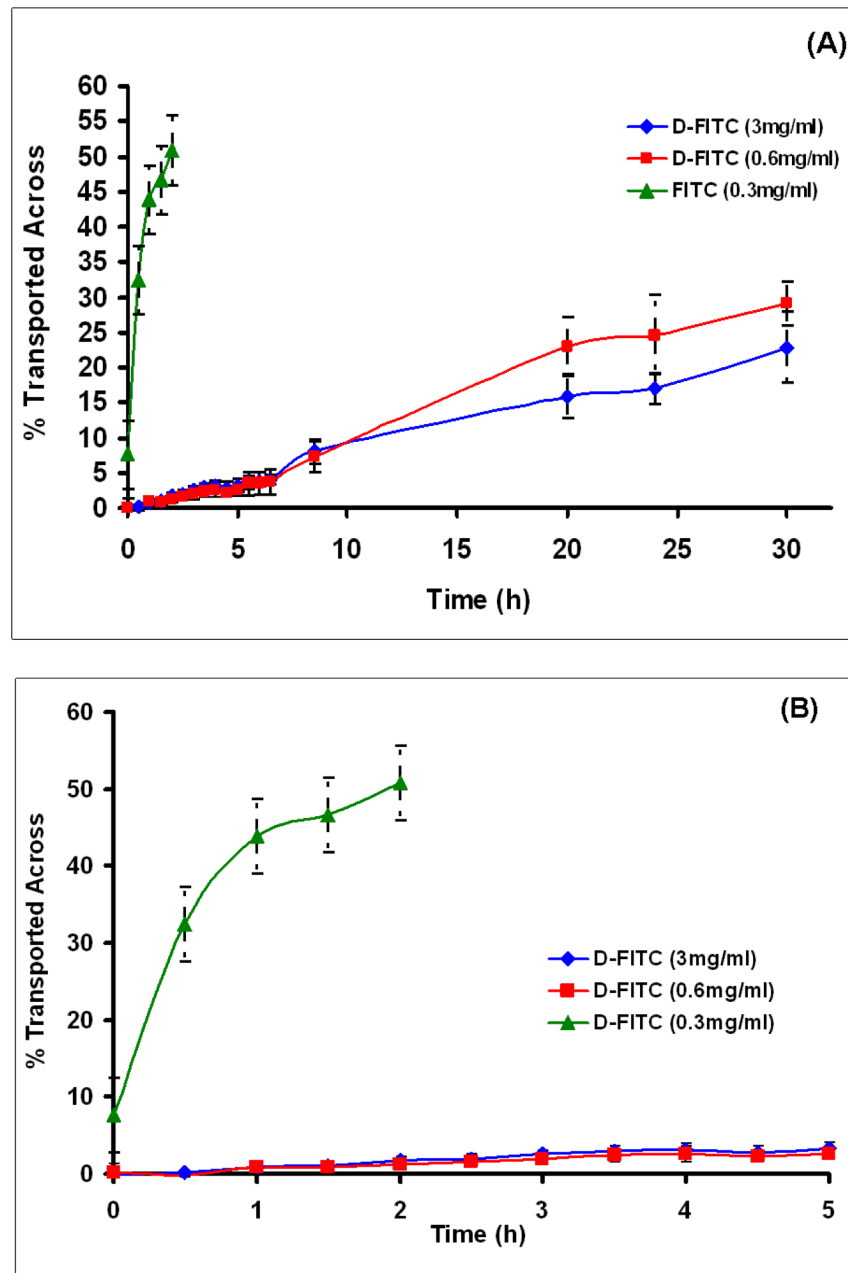


Fig. 4. (A) The transport of G_4 -PAMAM-O-GABA-NH-FITC (D-FITC) and FITC (unconjugated) across the chorion stripped off fetal membrane. The amnion was placed in the side by side diffusion chamber over 30 h to study the transport of dendrimers. (B) The FITC shows a rapid transport across the membrane (50 %) in 5 h, while the dendrimers show negligible transport of $\leq 3\%$ in 5 h. The concentrations of D-FITC studied were 0.6 mg/mL and 3 mg/mL. The concentration of FITC was 0.3 mg/mL.

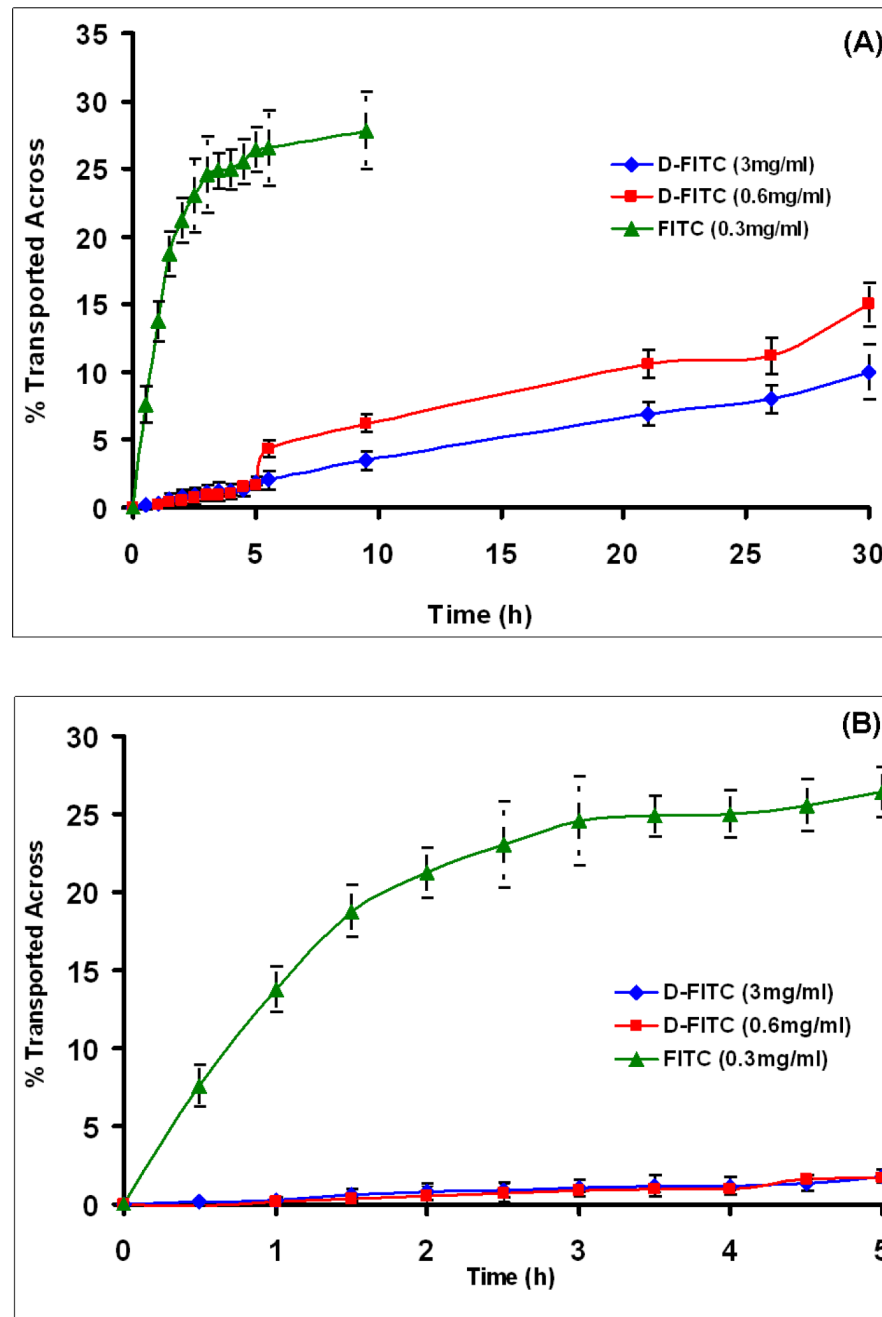


Fig. 5. (A) The transport of G₄-PAMAM-O-GABA-NH-FITC (D-FITC) and FITC (unconjugated) across the amnion stripped off fetal membrane. The chorion was placed in the side by side diffusion chamber over 30 h to study the transport of dendrimers. (B) The FITC shows a rapid transport across the membrane (~25 %) in 5 h, while the dendrimers show negligible transport of ≤ 3 % in 5 h. The concentrations of D-FITC studied were 0.6 mg/mL and 3 mg/mL. The concentration of FITC was 0.3 mg/mL.

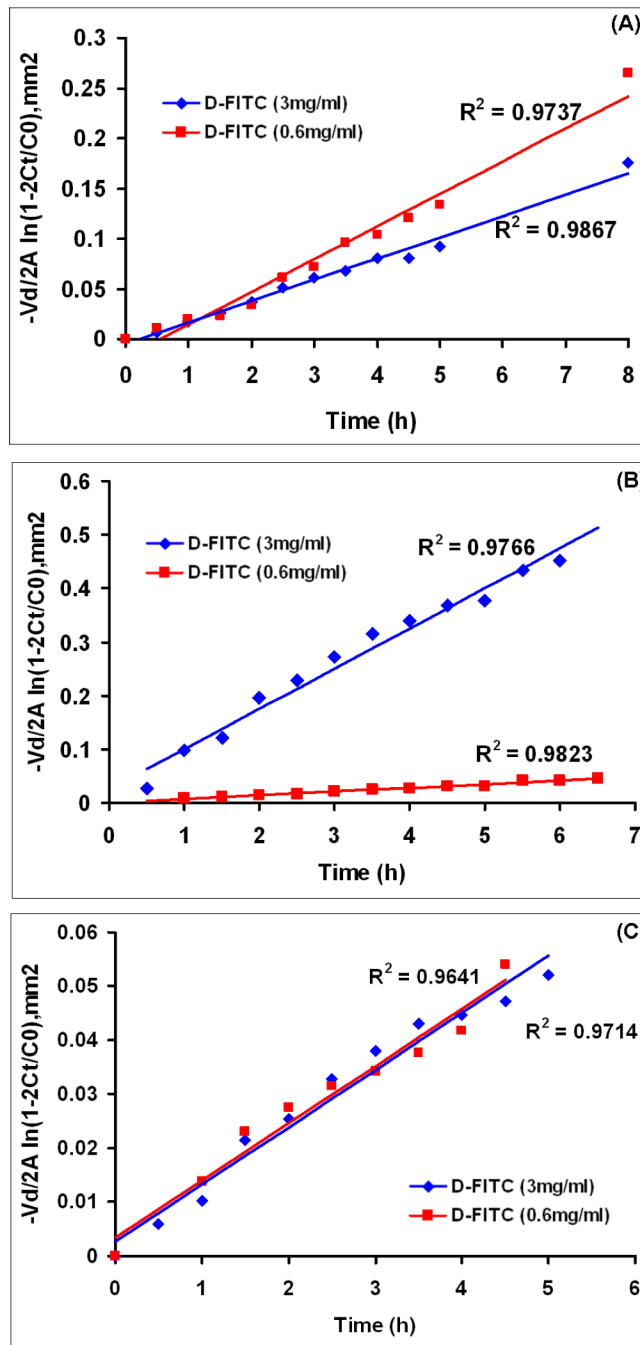


Fig. 6. Permeability coefficient for dendrimer measured across the (A) chorioamnion (B) amnion and (C) chorion. The concentrations of G_4 -PAMAM-O-GABA-NH-FITC (D-FITC) studied were 0.6 mg/mL and 3 mg/mL. The permeability coefficient of 0.6 mg/mL and 3 mg/mL D-FITC through (A) chorioamnion was 7.5×10^{-8} and 5.8×10^{-8} respectively (B) amnion was 1.86×10^{-8} and 2.08×10^{-7} and (C) chorion was 2.94×10^{-8} and $2.94 \times 10^{-8} \text{ cm}^2/\text{s}$

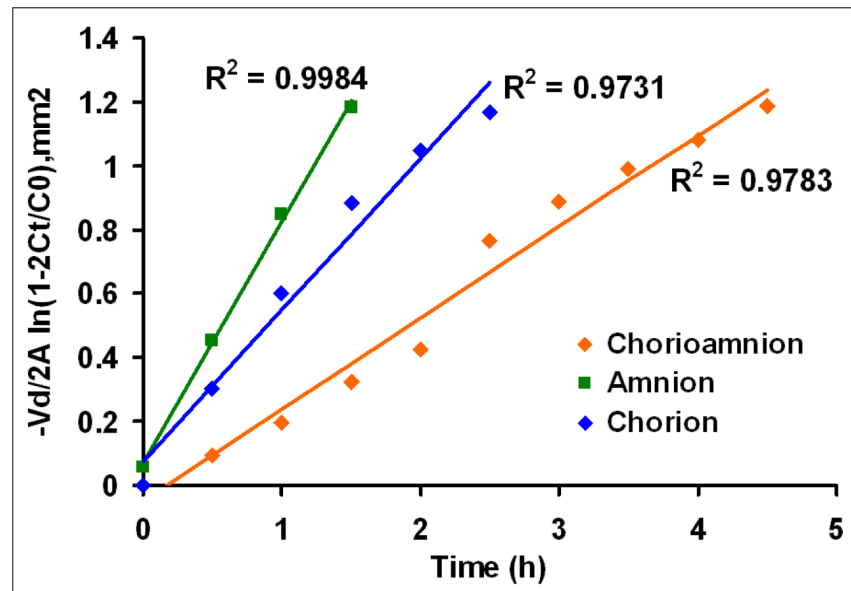


Fig. 7. Permeability coefficient for FITC (unconjugated) measured across the chorioamnion, amnion and chorion. The concentration of FITC was 0.3 mg/mL. The permeability coefficient of FITC through chorioamnion was 7.93×10^{-7} , amnion was 2.26×10^{-6} and chorion was 1.32×10^{-6} cm^2/s .

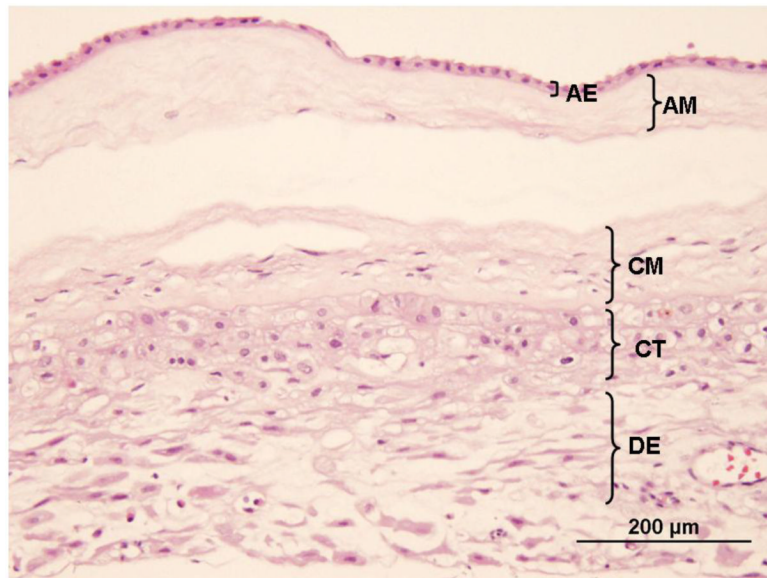


Fig. 8A.

The H and E stained human chorioamniotic (fetal) membrane. AE = amniotic epithelium, AM= amniotic mesoderm, CM=chorionic mesoderm, CT=chorionic trophoblast, DE=decidua comprising the stromal cells. For the transmembrane study the amniotic epithelium was placed facing the receptor cell to study the transport of dendrimer from maternal side (extra-amniotic cavity) to the fetal side.

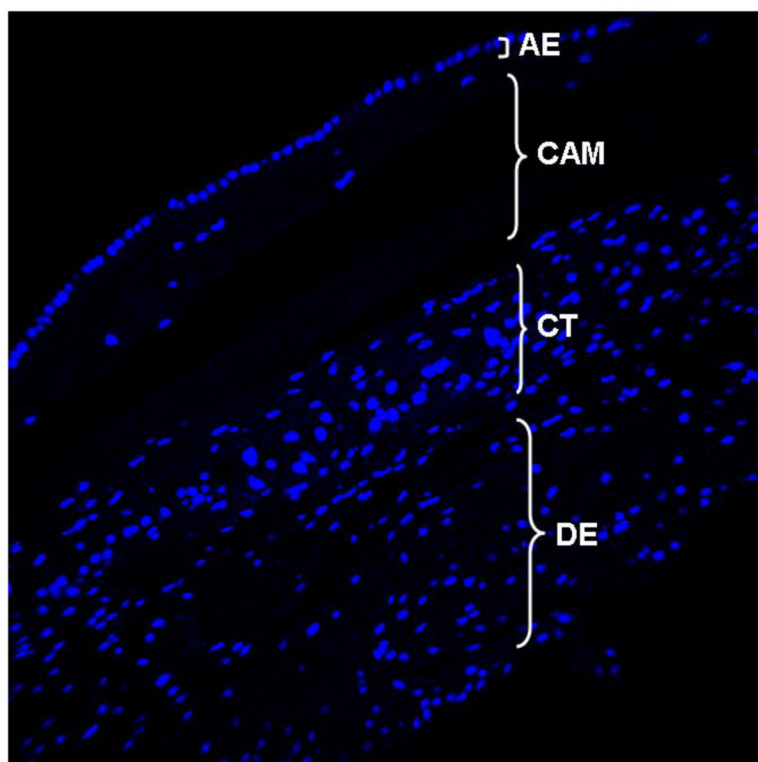


Fig. 8B.

The human chorioamniotic (fetal) membrane showing the nuclei stained blue with DAPI (control membrane without the treatment with G_4 -PAMAM-O-GABA-NH-Alexa (D-alexa) (20x). The negative controls rabbit isotype and mouse isotype replaced the primary antibodies. AE = amniotic epithelium, CAM = chorioamniotic mesoderm, CT = chorionic trophoblast, DE = decidua comprising the stromal cells. For the transmembrane study the amniotic epithelium was placed facing the receptor cell to study the transport of dendrimer from maternal side (extra-amniotic cavity) to the fetal side.

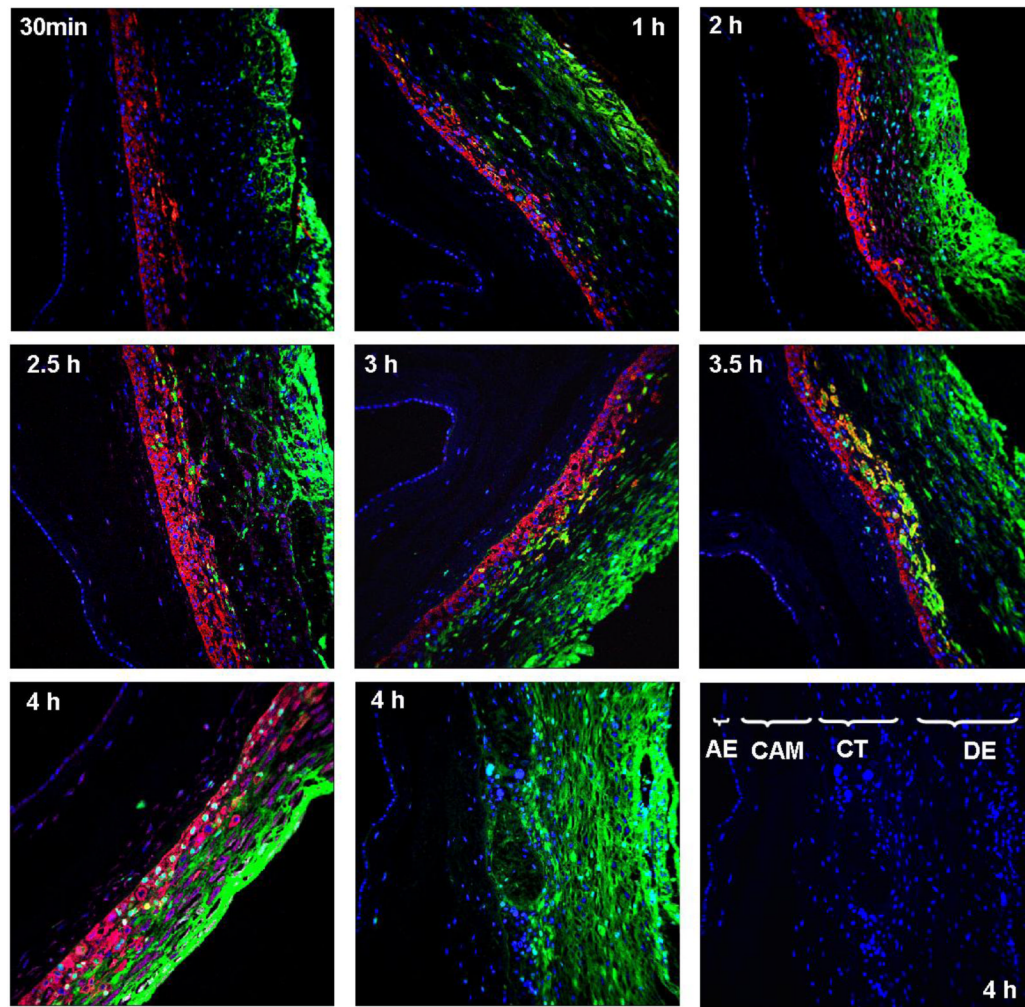


Fig. 9. Transmembrane transport of G₄-PAMAM-O-GABA-NH-Alexa (D-alexa) across the human fetal membrane at different time points (30 min, 1, 2, 2.5, 3, 3.5 and 4 h respectively) (20x). The nuclei are stained as blue (DAPI), the trophoblast cells in the chorion region are stained cytokeratin positive (red) and the stromal cells in the decidua are stained vimentin positive (magenta). The D-alexa (green) can be seen advancing through the different regions (the different regions are marked in the control membrane shown in bottom panel). At initial time points (30 min to 2 h) the dendrimer is seen in mostly in the decidua and stromal cells and at time points 3 to 4 h the dendrimers seem to diffuse into the chorionic trophoblast region. The image without cytokeratin and vimentin shows the diffusion of dendrimer throughout the decidua and trophoblast cells (4 h, bottom panel, center). AE = amniotic epithelium, CAM = chorioamniotic mesoderm, CT = chorionic trophoblast, DE = decidua comprising the stromal cells. For the transmembrane study the amniotic epithelium was placed facing the receptor cell to study the transport of dendrimer from maternal side (extra-amniotic cavity) to the fetal side.

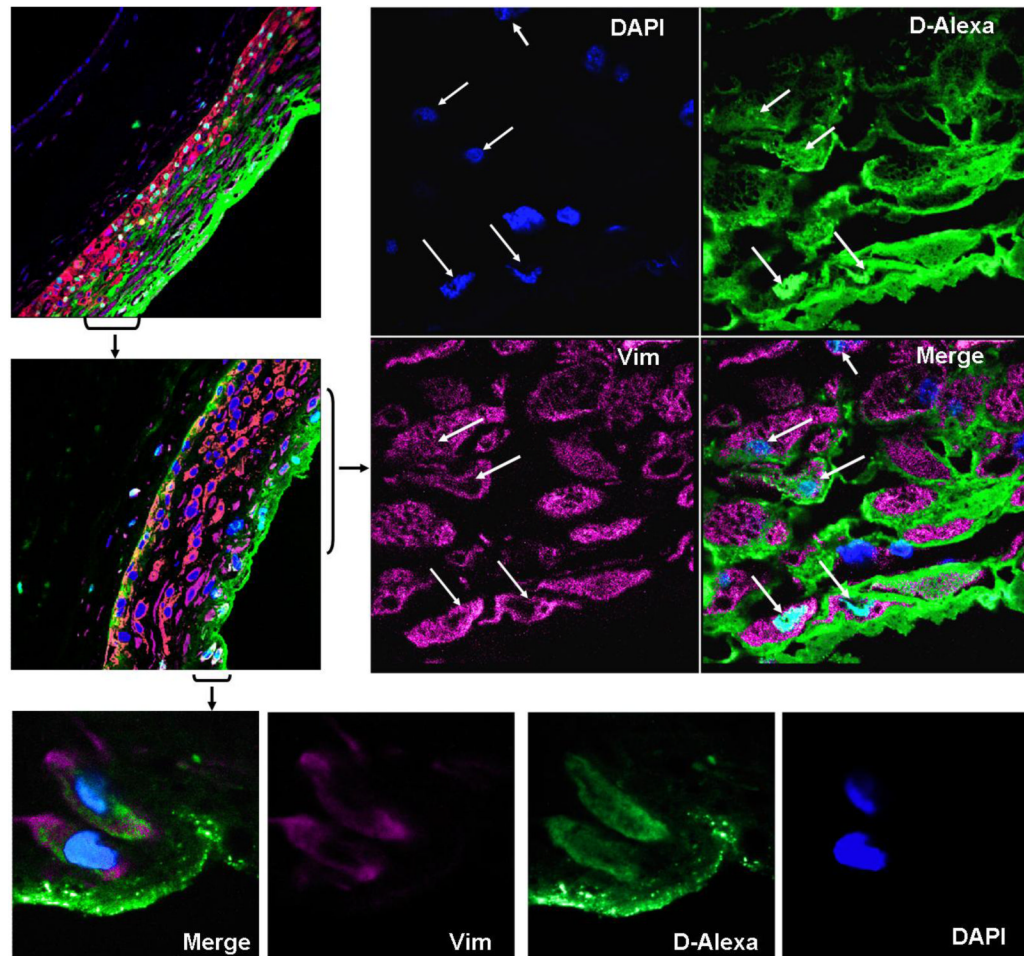


Fig. 10a.

The colocalization images for the G_4 -PAMAM-O-GABA-NH-Alexa (D-alex) in the decidual stromal cells at 4 h. The stromal cells are vimentin positive (magenta) and the nuclei of all the cells are stained blue. The D-alex is seen in green. The internalization of D-alex in the nuclei and cytoplasm of stromal cells can be seen from the merged composite image. The colocalized D-alex with nuclei appears as cyan (63x). The arrows identify the cells showing cellular uptake of dendrimer (63x). Also the dendrimer seems largely in the interstitial regions.

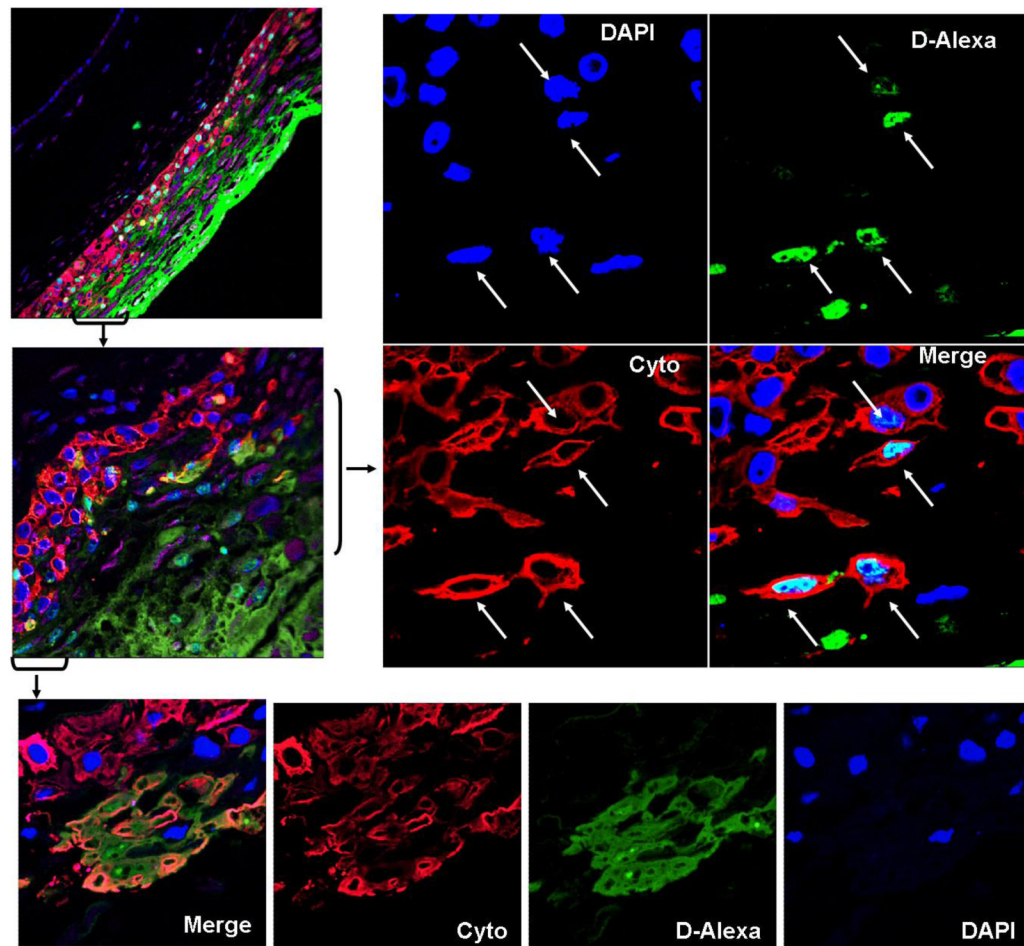


Fig. 10b.

The colocalization images for the G_4 -PAMAM-O-GABA-NH-Alexa (D-alex) in the chorionic trophoblast region at 4 h. The chorionic trophoblast cells are cytochrome positive (red) and the nuclei of all the cells is stained blue. The D-alex is seen in green. The internalization of D-alex in the nuclei of trophoblast cells is seen from the merged composite image. The arrows identify the cells showing cellular uptake of dendrimer. The colocalized D-alex with nuclei appears as cyan (63x). Also the bottom panel shows that dendrimer is largely in the interstitial regions (20x).

Table 1

Permeation coefficients of G4-PAMAM-O-GABA-NH-FITC (D-FITC) dendrimer and free FITC

Compounds	Permeability coefficients cm ² /s		
	Chorioamnion	Chorion	Amnion
D-FITC 0.6 mg/mL	7.5×10^{-8}	2.94×10^{-8}	1.86×10^{-8}
D-FITC 3 mg/mL	5.8×10^{-8}	2.94×10^{-8}	2.08×10^{-7}
FITC 0.3 mg/mL	7.93×10^{-7}	1.32×10^{-6}	2.26×10^{-6}